Characterization and Degradation of Polyhydroxyalkanoates (PHA), Polylactides (PLA) and PHA-PLA Blends

Rafeya Sohail
Microbiology and Molecular Genetics, University of the Punjab, Lahore
Nazia Jamil (nazia.mmg@pu.edu.pk)
Microbiology and Molecular Genetics, University of the Punjab Lahore

Research

Keywords: Degradation, FT-IR, Mixed Culture, PHA-PLA blends, Polyhydroxyalkanoates, Polylactides, SEM, Soil

Posted Date: December 1st, 2020

DOI: https://doi.org/10.21203/rs.3.rs-113670/v1

Characterization and Degradation of Polyhydroxyalkanoates (PHA), Polylactides (PLA) and PHA-PLA blends

Rafeya Sohail[1], Nazia Jamil[1*]

[1]Department of Microbiology and Molecular Genetics, University of the Punjab, Quaid-e-Azam Campus, Lahore 54590, Punjab, Pakistan

∗Correspondence:

Nazia Jamil

nazia.mmg@pu.edu.pk

Abstract

Biodegradable biopolymers such as polyhydroxyalkanoates (PHA) and polylactide (PLA) have wide range of applications in almost all sectors. Degradation of these polymers, however efficient, still creates a paradox with green chemistry principles. Blending of these polymers can potentially decrease plastic pollution due to their increased biodegradability. During this study, PHAwas produced using bacterial strains DL3; *Bacillus subtilis* (MT043898), PWA; *Bacillus subtilis* (MH142143), PWC; *Pseudomonas aeruginosa* (MH142144), PWF; *Bacillus tequilensis* (MH142145) and PWG; *Bacillus safensis* (MH142146). Corn-based PLA was produced chemically and physically blendedwith PHA (PHA-PLA blends). During molecular studies, PHA, PLA and PHA-PLA blendswere characterized via FT-IR analysis, SEM, and light microscopy indicating successful blending of PHA-PLA samples. FTIR results indicated PHA produced by strain PWF and mixed culture wasmcl-PHA. Degradation of polymers and copolymer blends was studied by bacteria for 12 weeks and in different environmental systems i.e. in soil, water, air, and heat for 20 weeks. Degradation analysis indicated highest degradation of PLA, followed by PHA-PLA blends. Among these systems, degradation was favored in soil (80%), followed by water (78%) and air (78%). Least degradation (76%) was observed on heat exposure. Sample degradation observed using light microscope and SEM showed fungal and bacterial colonization amidst cracks, crevices, bumps, and fractures after 20 weeks. Understanding the role of ambient microbial population during degradation and its impact on natural soil environment can be the focus of future studies.

Keywords

Degradation, FT-IR, Mixed Culture, PHA-PLA blends, Polyhydroxyalkanoates, Polylactides, SEM, Soil.

1 Introduction

Traditional fossil fuel and petrochemical based plastics have been a commodity since first production of plastics (Johnston et al 2017; Radecka et al 2016). The use of plastics has been increasing since they can be easily manipulated both chemically and physically to suit the current need (Reddy et al 2003). These properties have also made their use excessive and their eventual disposal irresponsible (Fossi et al 2020). In Europe, China and USA, plastic wastes account for 7%, 14% and 11.8% out of total generated municipal solid waste, respectively (Radecka et al 2016; Verma et al 2016; Johnston et al 2017).Biodegradable plastics are now being utilized as a suitable replacement of synthetic nondegradable plastics, in order to manage and control environmental pollution(Muniyasamy et al 2019).Biodegradable polymers can decompose in natural environment – within almost a year or less – to water, carbon dioxide, methane, biomass and inorganic compounds (Leja and Lewandowicz 2010). These degradation products can be utilized to enrich soil and/or as microbial metabolic substrates. Nevertheless, even biodegradable plastics are not a cure-all for the pollution caused by plastics (Narancic et al 2018). Many micro and nano particles are released during the degradation of biodegradable plastics (Sintim et al 2019). Home composting of many classes of biodegradable plastics cannot be achieved easily (Narancic et al 2018). Blending of different polymers – both synthetic and bio-based – to obtain various copolymers with desirable chemical and physical properties has become very versatile (Leja and Lewandowicz 2010). Recent studies have been conducted on utilization of

biodegradable polymer blends such as PHA-PLA blends, PLA/ starch composites, PLA-PCL blends, PHB-starch blends, PHB/P(HB-co-HV) blends, etc. (Muthuraj et al 2018; Shogren 2009).

Polyhydroxyalkanoates (PHA) have extensiveimport due to their biodegradability, biocompatibility, structural diversity, and efficient bio-friendly production using microorganisms(Li et al 2016). PHA are produced as carbon storage inclusion bodies by incorporation of hydroxy acid (HA) subunits. A single PHA molecule contains ~600 to 35000 *R*-hydroxy fatty acid subunits; where *R* is the side chain alkyl group (Tan et al 2014). *R* alkyl group can be a saturated, non-saturated, branched, or substituted alkyl group. Most studied and best characterized PHA is polyhydroxybutyrate, a homopolyester composed of *R*-3-hydroxybutyrate monomers (Koller et al 2015). The spectrum of PHA potentials ranges from applications as packaging films with various properties like UV resistance to high quality therapeutic or pharmaceutical materials like thermo-sensitive adhesives, carrier materials for controlled release of drugs *in vivo*, conduits guiding nerve repairs, implants, sutures, smart latexes, meshes, or a tissue engineering scaffolds etc. (Koller et al 2015; Koller 2018). The monomeric and oligomeric products of PHA degradation *in vivo,* do not cause toxicity or exert any negative effect on living cells, making them highly significant for medical field applications (Koller 2018). PHAs have been approved for clinical utilization in tissue engineering, biomedical devices, artificial organs and repair patches by United States Foods and Drugs Administration (USFDA) (Shah and Vasava 2019).

Polylactides (PLA), on the other hand, are aliphatic polyesters, produced from natural sources such as potato starch, wheat, corn, rice bran and biomass etc. (Shah and Vasava 2019; Ausejo et al 2018).Use of starchy source such as corn, wheat, beets, and potatoes etc. for PLA production utilizes 65% less energy, reduces generation of greenhouse gases by 68% and contains no toxins

(Muller et al 2017; Royte 2006; Rudnik 2019). Polylactides are highly transparent plastics with low processing temperature high elasticity modulus and high strength (Su et al 2019; Shah and Vasava 2019)making them a popular material in many industrial sectors (Msuya et al 2017). PLA, in fact, is also USFDA approved for applications in therapeutics and medical sectors (Shah and Vasava 2019). Thermoplastic PLA composed of lactidemonomeric units – synthesizedeither by direct polycondensation or ring-opening polymerization of lactides – can be grouped with aliphatic polyester family made from α-hydroxyl acids (Pretula et al 2016; Msuya et al 2017).Main constituent of PLA is a chiral monomer – existing in two enantiomeric forms i.e. L - and D- configurations – termed as 2-hydroxypropionic acid (Shah and Vasava 2019; Zhang and Thomas 2011; Kricheldorf 2001).

Blends of PHA-PLA show increased crystallinity, elasticity, thermal stability, and biodegradability (Roy and Visakh 2014; Msuya et al 2017; Zhang and Thomas 2011; Koller et al 2015; Su et al 2019). Biodegradative ability of biopolymers is strongly influenced by physiochemical nature of biopolymer i.e. stereoregularity, accessibility and crystallinity (Ray and Kalia 2017a). Copolymer blends of biodegradable thermoplastics like PHA and PLA only serve to enhance their potential for consumer applications (Rasal et al 2008).Biobased biodegradable PHA-PLA copolymer blends being biocompatible have potential applications in food, medicine, and agricultural sectors (Iwata 2015).Blending of PHA and high molecular weight PLA conducted previously reports that even though these blends show a defined interaction, these are not completely miscible(Zhang and Thomas 2011). Blending low molecular weight PLA with PHA could serve to enhance miscibility as well as biodegradability.

Current study was aimed at the production of PHA using previously isolated PHA producers. Corn based PLA having low molecular weight was produced chemically and biopolymers PHA

and PLA were blended physically. Biopolymers PHA, PLA and PHA-PLA copolymer blends were analyzed by light microscopy, scanning electron microscopy, and fourier transform infrared spectroscopy. Current study also addressed the degradation of these copolymer blends by bacteria and in different environmental systems i.e. soil, water, heat, and air.

2 Results

2.1 PHA, PLA and PHA-PLA Production

Solvent cast films of PHA were obtained after evaporation of chloroform. After 24 hours, highest biomass (12.91 g/L) on glucose was by PWC while highest PHA production (10.27 g/L; 84%) after 24 h was by strain PWF. PWC gave 7.73 g/L (60%) PHA production while PWF gave 12.30 g/L biomass. Highest percentage PHA production (87%; 9.28 g/L), however, was by mixed culture. Lowest biomass (5.07 g/L) and PHA production (1.94 g/L; 27%) were by strain PWG and DL3 respectively. Biomass and PHA production by strains DL3 and PWG were 7.10 g/L and 1.74 g/L (34%) respectively. Biomass and PHA production by strains PWA were 11.20 g/L and 4.42 g/L (39%). Biomass increased exponentially till 96 h, however % PHA production decreased after 48 h except in case of DL3. After 96 h, DL3 gave 22% (6.63 g/L) PHA production (**Table 1**).PHA films of PWA, PWC, PWF, PWG, DL3 and mixed culture on glucose were labelled as A, C, F, G, DL3 and M. Films thickness was approximately 1.5 mm. Transparent, thin films of corn based polylactide having 1.0 mm thickness were obtained. Films had a smooth texture however surface was slightly ridged due to pasting on aluminum foil. PHA-PLA blends (1:1) were obtained as solvent cast films with 1.5 mm film thickness. Blends were labelled as PA, PC, PF, PG, PDL3 and PM for PHA-PLA blends using PHA sample of PWA, PWC, PWF, PWG, DL3 and mixed culture, respectively.

Table 1PHA Production on Glucose				
Strains	**Time (hours)**	**Biomass (g/L)**	**PHA (g/L)**	**%PHA (%)**
PWA	**24**	11.20	4.42	39
	48	23.70	8.40	35
	72	37.50	10.43	28
	96	52.20	12.70	24
PWC	**24**	12.91	7.73	60
	48	18.41	10.73	58
	72	33.05	9.64	29
	96	49.91	12.82	26
PWF	**24**	12.30	10.27	84
	48	20.80	15.91	76
	72	39.40	13.94	35
	96	48.40	18.36	38
PWG	**24**	5.07	1.74	34
	48	11.03	2.92	26
	72	28.40	8.10	29
	96	41.17	9.04	22
DL3	**24**	7.10	1.94	27
	48	13.87	2.72	20
	72	28.37	6.23	22
	96	37.70	10.51	28
Mixed culture	**24**	10.66	9.28	87
	48	24.33	14.01	58
	72	41.67	14.52	35
	96	51.08	17.75	35

2.2 Characterization of PHA-PLA Blends

2.2.1 Fourier Transform Infrared (FT-IR) Analysis

FT-IR analysis of PHA, PLA and PHA-PLA gave a unique signature for each chemical complex in the sample within the FT-IR spectrum. Each spectrum was found to be a representative of sample's chemical composition, directly associated with concentration of chemical complexes.PHA sample of PWF showed absorption peaks at 1232.677, 1376.73, 1438.467, 1720.398, 2854.296 and 2928.38 cm^{-1} corresponding to C-O-C, CH_3,-CO-N-, C=O, -CH_2 and -CH_3 groups respectively (**Figure 1**).PHA sample of mixed culture showed absorption peaks at 1232.677, 1376.73, 1438.467, 1654.545, 1722.456, 2854.296 and 2928.38 cm^{-1}corresponding to C-O-C, CH_3,-CO-N-, C=O, C=O, -CH_2 and -CH_3 groups respectively (**Figure 2**). Absorption peaks in the range 605.02 cm^{-1} to 1115.37 cm^{-1} correspond to stretching vibrations of C-O and C-C. Absorptions at 1720.398 and 1722.456 cm^{-1} are known PHA marker bands corresponding to crystalline C=O group vibrations(Aljuraifani et al 2019).PLA sample shows peaks at 1232.677, 1376.73, 1438.467, 1654.545, 1745.092, 2854.296, 2928.38 and 3259.701 cm^{-1} corresponding to C-O-C, CH_3,-CO-N-, C=O, C=O, -CH_2 and -CH_3 and -OH groups (**Figure 3**). Absorptions at 1745.092 cm^{-1} correspond to amorphous C=O group vibrations. Absorption peaks in the range 605.02 cm^{-1} to 1016.599 cm^{-1} correspond to stretching vibrations of C-O and C-C.PHA-PLA sample of strain PWF (PF) showed peaks at 1232.677, 1376.73, 1438.467, 1654.545, 1720.398, 1745.092, 2854.296, 2928.38 and 3259.701 cm^{-1}corresponding to C-O-C, CH_3,-CO-N-, C=O, C=O, C=O, -CH_2 and -CH_3 and -OH groups (**Figure 4**). PHA-PLA sample of mixed culture (PM) showed peaks at 1232.677, 1376.73, 1438.467, 1654.545, 1722.456, 1745.092, 2854.296, 2928.38 and 3259.701 cm^{-1} corresponding to C-O-C, CH_3,-CO-N-, C=O, C=O, C=O, -CH_2 and -

142 CH_3 and -OH groups (**Figure 5**). Absorption peaks in the range 605.02 cm^{-1} to 1016.599 cm^{-1}
143 correspond to stretching vibrations of C-O and C-C.Absorptions at 1720.398 and 1722.456 cm^{-1}
144 correspond to crystalline C=O group vibrations while absorptions at 1745.092 cm^{-1} correspond to
145 amorphous C=O group vibrations. Percentage crystallization values calculated for samples PLA,
146 F, M, PF and PM were 21.8%, 28.8%, 27.7%, 33.7% and 25.2%, respectively. The presence of
147 both chemical complexes in PHA-PLA blendsas indicated by characterization results and the
148 increase in crystallization concluded the successful physical blending of these polymers.

149 ### 2.2.2 Microscopy and Elasticity

150 Light microscopy of PHA and PHA-PLA samples showed dark particlesagainst a light film
151 surface. Darker sites contained high concentration of particleswhile lighter areas contained low
152 concentration of particles. Micrographs of PLA samples showed no discernible small or large
153 particles, rather a smooth surface was observed. In PHA-PLA blends, the presence and size of
154 particles were significantly reduced. Samples of all PHA and PHA-PLA films showed surface
155 irregularities, varying in appearance and number with the variance in composition. Presence of
156 folds was also observed in all PHA samples indicating formation of folds during solvent casting
157 of PHA films. PHA-PLA samples showed red spots under natural light indicting a probable light
158 ionizing capability. These red spots disappeared on using in-built light bulb of microscope.
159 Crystal violet stained PLA samples showed that whole sample has been stained evenly. Surface
160 irregularities in PLA films appeared darker in contrast to smooth film surface. Crystal violet
161 stained PHA samples showed blue stained particlesagainst a light background. Almost all
162 particleshad been stained blue. In case of PHA-PLA blends, particlesas well as certain portions
163 of film (those containing PLA phase) had been stained blue. Due to increased uniform staining,
164 PHA-PLA blends appeared as brown or dark brown. On safranin stained PLA micrographs, spots

of red color were distributed homogenously across the film. On safranin staining, PHA and PHA-PLA samples appeared red against a light background. In case of PHA samples, film margins were observed as a darker red in contrast to the lighter red dye attained by film surface. In case of PHA-PLA samples, both margins and interior of film surface attained a uniform red coloration. Scanning electron microscopy of PLA samples showed typical regular fracture surfaces while those of PHA samples showed irregular fracture surfaces. PHA-PLA blends showed both fracture surfaces i.e. typical regular and irregular (**Figure 6**).Tensile strength measurement showed that low molecular weight PLA had lowest elasticity. PHA-PLA blends showed highest elasticity followed closely by PHA samples.

2.3 Degradative Analysis

2.3.1 Bacterial Degradation

During bacterial degradation only *Bacillus subtilis* degraded PHA, PLA and PHA-PLA films, while *Pseudomonas aeruginosa* had no effect.At week 2, PHA sample F, G, DL3, PLA sample, PHA-PLA sample PA and PDL3 were degraded. Highest degradation was of PHA sample G. bacterial growth surrounding degraded polymer changed color to transparent.At week 4, degradation rates followed the trend G>PDL3>DL3>PLA>F>PA>C>PG>PM. Bacterial growth surrounding degraded samples was milky in color,raised, bulbous and irregular (not in circular form). Bacterial growth around PHA samples had a lustrous sheen while growth surrounding PLA and PHA-PLA samples had no luster.Polymer color had changed to brown and edges had become irregular.At week 8, bacterial growth surrounding polymer had changed color to light brown and polymer edges had turned black. Degradation rates followed the pattern G>PDL3>PLA>DL3>PC>PA>C>F>PM.At week 12, bacterial growth surrounding samples had

187 turned dark brown. Degradation rates followed the same trend as at week 8. Overall highest
188 bacterial degradation was of PHA sample G.

189 2.3.2 Degradation in Different Environmental Systems

190 Morphologically all PHA, PLA, and PHA-PLA films were transparent and smooth initially but
191 gradually became rough in texture. Change in color of films also took place with time. At the end
192 of this study, all films had become rough and porous. Bacterial colonization of films was
193 observed in all cases. However, fungal penetration of films occurred only in case of water and
194 soil. As degradation prolonged, films become more prone to disintegration and fragmentation.
195 Molecular weight of films increased slightly at week 2 due to water uptake and then decreased
196 gradually. Percentage degradation followed the trend Soil > Water > Air > Heat.

197 2.3.2.1 Morphological Analysis of Samples

198 Soil degradation rates by PHA, PLA and PHA-PLA samples followed the trend
199 PLA>PF>PC>PM>PA>PG>F>C>M>A>G>PDL3>DL3 (**Figure 7**).Highest degradation rate of
200 approximately 80 % by PLA (0.0202 g) at week 20 was followed by degradation rates of PF, PC,
201 PM, PA, PG, F, C, M, A, G, PDL3 i.e. 68% (0.0316 g), 66% (0.0345 g), 66% (0.0345 g), 65%
202 (0.0345 g), 65% (0.0354 g), 61% (0.0391 g), 59% (0.0409 g), 55% (0.0450 g), 53% (0.0466 g),
203 49% (0.0512 g) and 46% (0.0536 g) respectively. Lowest degradation rate i.e. 31% was of PHA
204 sample DL3 whose weight decreased to 0.0687 g.

205 Water degradation rates by PHA, PLA and PHA-PLA samples followed the trend
206 PLA>DL3>PDL3>M>G>A>PG>PM>C>PA>PC>F>PF (**Figure 8**). Highest degradation rate of
207 approximately 78 % by PLA (0.0217 g) at week 20 was followed by degradation rates of DL3,

PDL3, M, G, A, PG, PM, C, PA, PC, F i.e. 66% (0.0340 g), 63% (0.0372 g), 63% (0.0371 g), 63% (0.0371 g), 62% (0.0381 g), 58% (0.0421 g), 56% (0.0440 g), 52% (0.0485 g), 50% (0.0501 g), 45% (0.0552 g) and 42% (0.0577 g) respectively. Lowest degradation rate i.e. 26% was of PHA-PLA sample PF whose weight decreased to 0.0739 g.

Air degradation rates by PHA, PLA and PHA-PLA samples followed the trend PLA>DL3>PDL3>G>M>A>PG>PM>C>PA>PC>F>PF (**Figure 9**). Highest degradation rate of approximately 78 % by PLA (0.0221 g) at week 20 was followed by degradation rates of DL3, PDL3, G, M, A, PG, PM, C, PA, PC, F i.e. 65% (0.0347 g), 62% (0.0379 g), 62% (0.0379 g), 62% (0.0378 g), 61% (0.0389 g), 57% (0.0429 g), 55% (0.0449 g), 51% (0.0494 g), 49% (0.0511 g), 44% (0.0562 g) and 41% (0.0588 g) respectively. Lowest degradation rate i.e. 25% was of PHA-PLA sample PF whose weight decreased to 0.0754 g.

Heat degradation rates by PHA, PLA and PHA-PLA samples in heat followed the trend PLA>DL3>M>PDL3>G>A>PG>PM>C>PA>PC>F>PF (**Figure 10**).Highest degradation rate of approximately 76 % by PLA (0.0241 g) at week 20 was followed by degradation rates of DL3, M, PDL3, G, A, PG, PM, C, PA, PC, F i.e. 62% (0.0378 g), 59% (0.0413 g), 59% (0.0413 g), 59% (0.0413 g), 58% (0.0424 g), 53% (0.0468 g), 51% (0.0489 g), 46% (0.0539 g), 44% (0.0557 g), 39% (0.0613 g) and 36% (0.0641 g) respectively. Lowest degradation rate i.e. 18% was of PHA-PLA sample PF whose weight decreased to 0.0821 g.

Highest degradation measured among all polymer and copolymer films under soil after 20 weeks (80%) was of PLA whose weight decreased from 0.1000 g to 0.0202 g. Transparent, smooth PLA sample at week 0 changed morphologically to slightly yellow, rough sample at week 10. At week 12, sample started to disintegrate slightly. At week 16, sample coloration changed to brown

and at week 20, sample disintegrated completely to powdered from on application of slightest pressure. Weight measurement showed a slight weight increase from week 2 (0.1363 g) to week 3 (0.1279 g), followed by a gradual decrease in weight up to week 20 (0.0202 g). Approximately 79 - 80 % of PLA sample was completely degraded by week 12. Degradation rates decreased after week 12 and remained almost same i.e. at 80 % up to week 20. Degradation by weight measured for PHA sample F was 61% with weight decrease from 0.1000 g to 0.0391 g. Transparent, smooth PHA sample F at week 0 changed to slightly yellow, slightly rough sample at week 5 with 0.0781 g weight and 22% degradation. At week 8, sample turned yellow and rough. Weight dropped from 0.0747 g at week 6 to 0.0664 at week 8 with 34% degradation. At week 10, 0.0584 g weight was measured with 42% degradation. At week 11, sample had started to lose its elasticity. Elasticity loss occurred gradually from week 9 to week 12, during which degradation rates slowed down. Degradation of 40% at week 9 was followed by 42% at week 10 and 11. At week 12, 44% degradation by weight of sample F has occurred. At week 16, sample coloration changed to brown and sample lost all elasticity turning brittle. At week 20, sample disintegrated on application of pulling force, having no noticeable elasticity. Weight measurement showed a gradual decrease in weight up to week 20 i.e. 0.0391 g. Approximately 61% of PHA sample F had been degraded completely by week 20. Among all PHA-PLA copolymer samples, highest degradation was by PHA-PLA sample PF (PLA blended with PHA of strain PWF). At week 2, 26% of sample had been degraded and weight had been reduced to 0.0737 g. By the 10^{th} week, 51% of sample had been degraded. Weight of degraded sample was recorded at 0.0503 g. During degradation, sample retained its initial morphology for 11 weeks. At week 12, transparent, smooth sample changed morphologically to a slightly yellow, slightly rough sample with 0.0429 g weight and 57% degradation. Sample turned yellow at week 16 with

0.0347 g weight and 65% degradation. At week 20, sample weight was recorded at 0.0316 g. Sample PF showed a maximum degradation rate of 68% after 20 weeks soil burial.

In case of air, water and heat, highest degradation was also by PLA. For PHA andPHA-PLA samples, highest degradation was achieved at week 20 by sample DL3 and PDL3, respectively. In air, degradation of DL3at week 20 was 65%, when sample weight had dropped down to 0.0347 g. Initially, sample started as transparent and smooth. During week 2, sample became cream colored and sample weight decreased to 0.0809 g. At week 3, sample turned slightly rough. Up to 22% of sample had been degraded and sample weight decreased to 0.0782 g. Sample changed color to yellow at week 6. Sample weight of 0.0722 g was recorded. A degradation rate of 28% was measured.At week 9, sample become rough. Sample had degraded up to 45% with an average weight of 0.9552 g. At week 16, sample turned brownish.PHA-PLA sample DL3 showed 62% degradation with 0.0379 g weight at week 20. Sample changed color to cream with 25% degradation and 0.0753 g weight at week 7. Sample showed 34% degradation with 0.0659 g weight at week 9. Sample had turned slightly rough with yellow coloration. At week 12, sample coloration had changed to brownish yellow with 0.0550 g weight and 45% degradation.

2.3.2.2 Microscopic Analysis of Samples

2.3.2.2.1 Light Microscopy

Air degraded PHA and PHA-PLA samples showed minimal bacterial colonization. Samplesurface was riddled with cracks, crevices, and bumps. Heat degraded PHA and PHA-PLA samples were observed as burnt with dark brown coloration against a light background except in

case of PLA sample. PLA sample showed more pronounced surface roughening as compared to other samples. No bacterial colonization was observed.Soil degraded PHA and PHA-PLA samples showed bursting and swelling due to bacterial colonization. PLA sample showed completely degraded surface morphology. Fungal hyphae were observed penetrating and colonizing the PLA sample. Fungal hyphae were absent in case of PHA and PHA-PLA samples. All water degraded PHA and PHA-PLA samples showed bacterial colonization causing swelling in polymers. PLA sample of water also showed presence of fungi penetrating sample. Bacterial and fungal colonization of sample was also observed.

2.3.2.2.2 Scanning Electron Microscopy

SEM micrographs of polymer films before degradation showed typical fracture surfaces. Distinctive features of degraded polymer films were observed on SEM microscopy after week 20 of soil burial (**Figure 6**). PHA sample of strain PWF before degradation showed typical fracture surfaces and light reflecting particlesat 500 X and 1000 X. At 2000X and 3000 X, irregular surface morphology was observed. SEM micrographs of sample after degradation showed presence of degradedparticles, crevices, cracks, bursts, and bacterial colonization. At 500 X, bacterial colonization of sample surface was apparent while at 1000 X, sample showed irregular fracture surfaces riddled with bumps and swells. At 2000 X, cracks and crevices were observed between bumps and swells of sample. At 3000 X, small pieces of samples were observed to be breaking down and off.

SEM micrographs of PLA sample before degradation showed an almost smooth surface having regular fracture surfaces. PLA sample after degradation showed both bacterial and fungal colonization of polymer surfaces. At 500 X, a webbed colonization pattern was observed

encompassing, the sample. Fungal hyphae were further observed to penetrate the polymer. Presence of pits, depressions, bumps, cracks, crevices, and swells was also apparent at 500 X, indicating highest degradation in PLA sample. At 1000 X, polymer was observed to be breaking off into small pieces. At 2000 X, these small pieces of sample were seen to be held together due fungal penetration and webbed bacterial colonization. SEM micrograph of PLA sample at 3000 X, showed these small pieces as broken off small budding spheroids with irregular surfaces.

PHA-PLA sample before degradation showed a smooth surface riddled irregularly with a rough surface at 500 X i.e. regular fracture surfaces of PLA are more apparent. At 1000 X and 2000 X, small depressions and pits were observed indicating overlay of both polymeric fracture surfaces.At 3000 X, at the site of pits and depressions, irregular fracture surfaces typical of PLA were observed. After degradation, SEM micrographs of PHA-PLA sample at 500 X showed a branching colonization of sample. Sample surface was observed to be irregular having pits, depressions, cracks, and cervices. No bumps or swells were observed. At 1000 X, numerous small broken pieces of sample were observed. Large pieces were also seen to be breaking down. At 2000 X and 3000 X, sample surface was observed as being comprised of broken fragments adhering to each other.

3 Discussion

Polyhydroxyalkanoate (PHA) was produced using previously isolated PHA producers (Sohail and Jamil 2019; Sohail et al 2020).Polylactide (PLA) was produced using corn starch and solvent cast PHA-PLA films were obtained after solvent induced recrystallization. PLA-PHA blends showed improved elasticity since blending with PHA enhances crystallinity of PLA. This property is attributed to the crystalline behavior of PHA which acts as filler in copolymer blends

318 to enhance PLA matrix. There might also be strong interfacial bonding between these polymers,
319 however no definitive tests were performed to ascertain this bonding. Highly crystalline property
320 of PHA also improves mechanical properties since in PLA-PHA blends, PHA acts as filler as
321 well as nucleating agent. Similar findings were reported by Zhang *et al.* who studied effect of
322 PLA-PHB blends on thermal, mechanical and biodegradation properties (Zhang and Thomas
323 2011).

324 In both PHA samples, stretching vibrations of crystalline carbonyl group (C=O) for were found
325 at 1720.398 cm^{-1} and 1722.456 cm^{-1},while in PLA sample, stretching vibrations of amorphous
326 carbonyl group (C=O) for were found at 1745.092 cm^{-1} (**Figure 1-3**). FT-IR analysis of PHA
327 polymer confirms the presence of PHA functional group. Munir *et al.*have reported production of
328 mcl PHA by *Bacillus subtilis*, *Pseudomonas aeruginosa* and co-cultures on glucose(Munir and
329 Jamil 2018). Masood *et al.*also reported production of mcl and lcl PHA by *Bacillus* sp. on
330 glucose and olive oil, respectively (Masood et al 2017). Results of characterization and literature
331 review indicate that mcl PHA is produced.In case of PHA-PLA blends, both absorption bands
332 were observed due to blending of both polymers (**Figure 4, 5**).Zhang *et al.* reported similar
333 results for FT-IR spectrum of PLA showing strong absorption bands at 1745 cm^{-1} related to
334 vibration of amorphous carbonyl groups, and weak absorption bands at 1755 cm^{-1}(Zhang and Thomas
335 2011). The absorption spectra of corn based PLA are very similar to those reported by Basnet *et*
336 *al.*, who found FT-IR, TGA and DSC test results of corn based PLA similar to those of reference
337 PLA (Basnet and Wiberg 2016). The compositional analysis of the polymer is just a
338 confirmation of the PLA functional group, and notan exploration of potential new physical or
339 chemical characteristics. However, the process and/or polymer can be physically or chemically
340 modified.Zhang *et al.* also reported FT-IR spectra of PHA showing strong absorption bands at

1718 cm^{-1} related to crystalline carbonyl stretching vibrations and weak absorption bands at 1740 cm^{-1}. They reported two strong bands at 1722 cm^{-1} for crystalline carbonyl and 1745 cm^{-1} for amorphous carbonyl in PHA-PLA blends(Zhang and Thomas 2011).Absorption bands were also observed at 3259.701 cm^{-1} assigned to stretching vibrations of -OH group. Absorption bands corresponding to lateral monomeric units of aliphatic asymmetric alkyl groups were observed at 2854.296 and 2928.38 cm^{-1}. Absorption bands corresponding to stretching vibration of carbonyl ester groups were observed at 1654.545 cm^{-1}. Absorption bands corresponding to intracellular amide groups were observed at 1438.467 cm^{-1}. Absorption bands corresponding to stretching vibrations of terminal alkyl groups were observed at 1376.73 cm^{-1}. Absorption bands corresponding to asymmetric C-O-C groups were observed at 1232.677 cm^{-1}. Ismail *et al.* also reported presence of C=O, C-H, C-O, and O-H absorption bands indicating bioplastic formation (Ismail et al 2016).

Aljuraifani *et al.* also reported similar absorption bands i.e. strong absorption band at 3456.43 cm^{-1} corresponding to stretching vibrations of hydroxyl group, bands at 2986.44 and 2858.50 cm^{-1} corresponding to aliphatic alkyl groups, bands at 1637.56 cm^{-1}corresponding to C=O and at 1261.44 cm^{-1}corresponding to stretching vibrations of C-O group (Aljuraifani et al 2019). Percentage crystallization values calculated for samples PHA, M, PM were 21.8%, 27.7% and 25.2%, respectively.Zhang *et al.* reported that the typical degree of crystallinity for PHA is about 10.2% which can be increased up to 60% under high pressure crystallization (Zhang et al 2012). Gopi et al. reported 26.4% degree of crystallization in poly-3-hydroxydodecanoate (P3HDD) (Gopi et al 2018) while Yang also reported 22.75% degree of crystallinity for PHA (Yang 2014). Defined increase in crystallization was observed in case of sample PF i.e. 33.7% where samples F and PLA had 28.8% and 21.8% crystallization respectively.Rasal et al. reported 20% increase

364 in crystallinity of PLA PHA-g-PAAmand PAAm after solvent induced crystallization (Rasal et al
365 2008). Comparatively, values of %crystallinity reported by Nerker *et al.* – on DSC of PHO, PLA
366 and PLA/PHO blends - were 24% for PLA, PHO (Polyhydroxy octanoate) and 16% for
367 PLA/PHO blend (Nerkar et al 2015). FT-IR results indicated that in PHA-PLA blends, particles
368 of PHA and PLA are distributed uniformly across the dried films of copolymer. These results
369 also account for the fact that in PHA-PLA blends, crystallizationof PLA is increased. In light
370 microscopy, absence of aggregates in PLA samples indicates that PLA is amorphous while in
371 contrast presence of aggregates andparticles in PHA samples is due to its crystallinity. In case of
372 PHA-PLA blends, PLA being amorphous reduces the presence and size of particles in crystalline
373 PHA significantly. In a study by Zhang *et al*., similar findings were reported i.e. crystalline PHB
374 dispersed in continuous phase of amorphous PLA. Zhang *et al*. reported lowering in rate of
375 crystallization due to reduction in size and number of PHB spherulites, to the extent that
376 crystalline phase of PHB became continuous (Zhang and Thomas 2011). In scanning electron
377 microscopy, presence of typical fracture surfaces in PLA samples are due to its amorphous
378 nature while PHA samples show the irregular fracture surfaces indicative of a crystalline
379 polymer. In PHA-PLA blends, both types of fracture surfaces were observed which showed that
380 PHA particles are distributes across amorphous PLA as fillers. Zhang *et al*. reported presence of
381 two phases in PHA-PLA blends using high molecular weight PLA, accounting for the fact that
382 those PHA-PLA blends were not miscible (Zhang and Thomas 2011).Overall, characterization
383 results indicated that although PHA and low molecular weight PLA polyesters were miscible, no
384 discernible strong molecular interactions were found between these two polymers. However,
385 there was a defined interaction between PHA and PLA particles. This interaction resulted in
386 increased elasticity, crystallinity, changes in mechanical properties.

Many microbes have the ability to degrade PHA, however enzymatic degradation of biopolymers also takes place in natural ecosystems. The effects of bacterial degradation by *Bacillus subtilis* and *Pseudomonas aeruginosa* on PHA, PLA and PHA-PLA blendswithout the interfering effects of enzymatic degradation were studied in aseptic conditions. Blends of PLA-PHA also showed increased biodegradability in differentenvironmental systems i.e. air, water, soil, and heat. Highest degradation was observed in soil (**Figure 7**), followed by degradation in water (**Figure 8**) and then air (**Figure 9**). Lowest degradation rates were observed on application of heat (**Figure 10**).Following the overall degradation pattern, highest degradation was of PLA, followed by PHA-PLA blends and lowest degradation was of PHA samples. Discoloration of samples occurring with increasing time also accounts for their degradation. There was an initial increase in weight at the beginning of experiment attributed to the absorption of water by PHA, PLA and PHA-PLA blends. Increase in weight was especially defined in case of corn-based PLA and PHA-PLA blends. This can be attributed to the fact that the building blocks of PLA are hydrophilic. However, Zhang *et al*. reported increased water absorption by PHB compared to synthetic PLA and lowered PLA degradation rate at room temperature (Zhang and Thomas 2011).Since, this study was conducted in uncontrolled environments, the richness of microbial flora and other environmental properties could have affected the trend of degradation. Differences from consistent degradative behavior can also be due to dissimilarity of PLA class i.e. PLA synthesized by direct polymerization is more amorphous and has a more easily degradative chemical nature as compared to PLA synthesized by ring polymerization.Biodegradation patterns of polymer understudy could be due to their physical form. Volova *et al.* reported high degradation of PHA polymer films compared to compacted pellets of same weight and chemical composition in seawater. However, unchanged degree of

410 crystallization was reported i.e. both amorphous and crystalline phases disintegrated equally
411 (Volova et al 2010).

412 Lowest degradation of polymer sample at 37℃ indicates that these biopolymers are
413 biocompatible. However, polymer degradation has been reported to take place at high
414 temperatures. Sarasa *et al.* reported 63.6% biodisintegration of pieces made of PLA with
415 foaming agent and 79.7% biodisintegration degree in pieces made of PLA-corn(Sarasa et al
416 2009). Slow degradation at in heat and in water also indicates the probable applications of these
417 biopolymers as medical implant devices, drug carriers, tissue engineering etc. (Modjarrad and
418 Ebnesajjad 2013; Zinn et al 2001). Water soluble and/or biodegradable also have significance in
419 therapeutics and medical physiology (Li and Loh 2015). Results indicate that air degraded
420 polymer samples had become a site for microbial colonization. Degradation in air was mainly
421 due to microbial flora circulating through. The ambient environment for PHA degradation in soil
422 was loam category having more moisture, humus, nutrients, and diverse soil biota, indicating
423 increased fertility. The effect of ambient environment on PHA, PLA and PHA-PLA polymers
424 investigated by soil-burial tests showed that degradation of PLA films was highest and remained
425 almost constant after weight reduction from 0.1 g to 0.02 g at 20 weeks. PHA-PLA
426 blendsfollowed these degradative rates closely. While comparative degradative ability of PHA
427 was lowest among all samples. Corn based PLA and PHA serves as carbon source for soil
428 microbiota. Among these PLA is most easily available and accessible to microorganisms as it
429 can be degraded both at the surface and under the surface enzymatically. High degradation of
430 PLA may also be due to its amorphous nature. Modal *et al.* reported 88% weight loss in
431 starch/sucrose composite films within 30 days of soil burial (Mondal 2015). Marichelvam *et al.*
432 reported 48.73% biodegradability in corn derived bioplastics after placement in soil at 3 cm

depth for 15 days (Marichelvam et al 2019). PHA, on the other hand, was degraded on the surface. It was speculated that rapid degradation of PHA films, while being high, was comparatively lower since depolymerase enzymes only acted on the surface. Ong *et al.* reported almost complete degradation of 0.03 mm PHA films after 8 weeks in soil (Ong and Sudesh 2016). However, among PHA samples degradation of mixed sample PHA (PM) was highest indicating that it is also possible degradation of pure PHB homopolymer having higher crystallinity was lower as compared degradation of comapartively less crystalline PHB heteropolymer. Ong *et al.*also reported faster degradation of P(3HB-co-21 mol% 3HHx) as compared to P(3HB)(Ong and Sudesh 2016).Degradative ability of PHA-PLA blends can therefore be high compared to PHA, as PLA phase is degraded, unveiling underlaying PHA phase for degradation both on and under the surface. It is also possible that diverse microbiota of soil environment degraded PHA by action of depolymerases extracellularly as well as intracellularly by absorbing PHA granules. In degradative studies, it has been reported that intracellular n-PHB depolymerase of *Bacillus megaterium* also exhibits extracellular activity (Ray and Kalia 2017a).Previous studies have also reported that for polymer blend degradation additive rule cannot be applied often. Thus making it difficult to predict polymer blend degradation pattern based on the degradative behavior of pure components (La Mantia et al 2017).

SEM micrographs of PHA, PLA and PHA-PLA copolymer after degradation in soil showed the presence ofdistinctive depolymerized fracture surfaces. Bacterial colonization of PHA, PHA-PLA samples and additional fungal penetration of PLA samples leading to bursting and swelling, probably aided in release of smaller molecules and/or short molecular chains capable of passing through outer cell membranes. Ong *et al.* reported similar findings while studying effects of PHA

degradation. They also attributed weight loss to bacterial and fungal colonization (Ong and Sudesh 2016).PLA sample was shown to be degraded as a whole, indicating a nonenzymatic degradation by hydrolysis.While presence of bacterial colonies and fungal hyphae on films indicated an enzymatic degradation and uptake of degraded products. PHA sample, on the other hand, showed occurrence high degradation at sample surfaces indicating an enzymatic degradation following bacterial colonization. Ong *et al*. also reported catalytic action of depolymerase enzymes on porous sample surfaces already degraded by surface erosion (Ong and Sudesh 2016). PHA-PLA blends showed increased degradation compared to PHA, but decreased degradation compared to PLA, accounting for the fact that both enzymatic and nonenzymatic degradation occurred in the copolymer blends. SEM micrographs of PHA-PLA blends show that erosion across the surface is due to PHA particles and degradation within the film structure is due to PLA particles. Decreased degradation rate compared to PLA can be due to the uniform distribution of PHA crystals across the PLA matrix. These PHA crystals can be degraded by various surface enzymes but only after the overlaying PLA matrix has been degraded nonenzymatically.

4 Conclusion

PHA-PLA blends show significant degradation.Physical blending of biologically produced PHA using previously isolated PHA producers with chemically produced corn based PLA significantly enhanced degradative ability of resulting blends. Biopolymers PHA, PLA and PHA-PLA blends have significance in environmental studies as well as industrial sectors. Knowing the impact of natural soil environment on biodegradable biopolymers will aid in understanding the role of ambient microbial population in degradation. Degradation in different

systems also opens new avenue of research to explore metabolic pathways of ambient polymer degrading bacteria. Future studies can be focused on the effect of such degradative behaviors on environment i.e. on soil fertility, irrigation water, etc.

5 Materials and Methods

5.1 Revival of Stock Cultures

Stock cultures of bacterial strains PWA; *Bacillus subtilis* (MH142143), PWC; *Pseudomonas aeruginosa* (MH142144), PWF; *Bacillus tequilensis* (MH142145), PWG; *Bacillus safensis* (MH142146), and DL3; *Bacillus subtilis* (MT043898) were taken from Research Lab II, MMG (Sohail et al 2020; Sohail and Jamil 2019) and revived by culturing at 37℃ on Nutrient Agar for 24h. Fresh cultures were maintained by streaking discrete colonies on Nutrient Agar and incubating for 24 hours at 37℃.

5.2 Polyhydroxyalkanoate Production

Polyhydroxyalkanoate (PHA) detection media supplemented with 2% glucose as carbon source was used for cultivation of PHA producers (Chaudhry et al 2011; Javaid et al 2019; Rehman et al 2007). Preliminary 10% bacterial culture was added aseptically to 200 ml media dispensed in 500 ml Erlenmeyer flasks and incubated at 37℃ for 96 hours in a rotary incubator. Using IRMECO U2020 UV-Vis spectrophotometer, optical densities were recorded at 600 nm (Teeka et al 2010). Culture media (40 ml) was collected at 24, 48, 72 and 96 hours, and centrifuged at 6000 rpm for 15 minutes to obtain cell biomass. Cell biomass was measured in grams. PHA produced by bacterial cells was extracted from biomass by SDS/ Sodium hypochlorite digestion

and subsequent incubation in chloroform (Van Doan et al 2015). Pellet was treated at 25℃ and pH 10.0 for 15 minutes with 0.25% SDS then for 5 minutes with 5.25% sodium hypochlorite and centrifuged at 6000 rpm for 15 minutes. Pellet was washed using ice cold acetone, centrifuged again at 6000 rpm for 15 minutes and transferred to 100 ml glass Erlenmeyer flask. Chloroform (10 volumes) was dispensed in flasks and incubated at room temperature for 48 hours. Chloroform/PHA mixture was filtered using Whatman Grade 1 filter paper to remove cell debris. Chloroform was evaporated to obtain solvent-cast dry films of PHA under a fume hood (Sohail et al 2020; Sohail and Jamil 2019). Dry weight PHA films was recorded in grams (Van Doan et al 2015). Percentage of PHA was calculated using formula:

$$\% PHA = \frac{Weight of PHA}{Weight of biomass} X\ 100$$

5.3 Corn based Polylactide Production

Corn starch was used for chemical production of corn-based polylactide (Keziah et al 2018; Marichelvam et al 2019; Muller et al 2017). Corn starch (9.5 ml) was charged in 60.0 ml of cold deionized water (DI), 0.1M HCl (2.0 ml), glycerin (5.0 ml) used as plasticizer and 5% acetic acid (5.0 ml) and stirred vigorously until a uniform solution was prepared. Hot plate with magnetic rotor was preheated to 120℃ temperature for 10 minutes. Solution was placed on hot plate under fume hood to avoid fumes, stirred vigorously and temperature was increased gradually to 145℃ over 20 – 25 min. Mixture was stirred manually and agitated continuously till a clear, homogeneous, gelatin-like suspension was formed(Basnet and Wiberg 2016). This semi solid suspension was poured on aluminum foil sheet and spread uniformly using glass rod to make a film. Cast film was air dried for 3-4 days to remove moisture (EstructuraProteinas 2020; Green Plastics 2012; Rudnik 2019; Solomonides 2016).

5.4 Production of PHA-PLA Blends

PHA polymer (0.05 g) was dissolved in chloroform (5.0 ml) and air dried until 0.1 ml chloroform remained. PLA polymer (0.05) was dissolved in hot distilled water (5.0 ml) at 65℃ and volume was raised up to 19.9 ml. Distilled water containing PLA (19.9 ml) was dispensed in chloroform containing PHA (0.1 ml) at 25℃and mixed thoroughly to obtain 1:1 PHA-PLA blend (Kirchnerová and Cave 1976; Karaffa 2013; Mackay et al 1980). Solution was dispensed in glass vial, dried by evaporation with constant shaking at 25℃. Final PHA-PLA blend of 0.1 g weight was obtained as film.

5.5 Characterization of PHA, PLA and PHA-PLA Blends

Analyzation of structure, fracture surfaces, crystallinity, and identification of organic functional groups of PHA, PLA and PHA-PLA blends were done using light microscopy, scanning electron microscopy, FTIR spectroscopy, and tensile strength measurement. Light microscope, LABOMED, was used to analyze structure of PLA, PHA and PHA-PLA blends. Light micrographs were taken using IRMECO camera. For further clarification of sample morphology, samples were stained using 10% dilution of crystal violet and 10% dilution of safranin for 1 minute. Samples were flooded with dye for 1 minute, washed using distilled water and air dried. Unstained, crystal violet stained, and safranin stained samples were observed using 4 X, 10 X, 40 X and 100 X magnification. Tensile strength of polymers was measured by calculating stress. Scanning electron microscope, EVO LS 10, used to analyze morphologic characteristics i.e. structure, crystallinity, fracture surfaces etc. of PLA, PHA and PHA-PLA blends, was operated at 20.0 kV acceleration voltage. Scanning electron microscopy was conducted at Central Research Lab, Lahore Women's University. Samples were observed at 500 X, 1000 X, 2000 X

and 3000 X magnification under low vacuum (80 Pa) using Zeiss SE microscope.FT-IR analysis was used to inspect presence of functional organic groups in PHA, PLA and PHA-PLA samples. FT-IR absorption spectra were obtained at room temperature using SHIMADZU IRTracer-100. FT-IR scan range was 4000 cm^{-1} to 400 cm^{-1}. Resolution of 4 $cm^{-1}$was used to record all spectra for an average of 64 scans. Data analysis was done using GRAM/AI software and percentage crystallinity of polymer material was evaluated using the method suggested byZerbi(Zerbi et al 1989).

$$\% \text{ Crystallinity} = 100 - \left[1 - \frac{\frac{Ia}{1.2333Ib}}{1 + (\frac{Ia}{Ib})}\right] \times 100$$

where *Ia* and *Ib* are the absorbance values determined from the bands at (PLA) 1745$cm^{-1}$and 1845 cm^{-1}, (PF, M) 1732$cm^{-1}$and 1832 cm^{-1}, (PM) 1730$cm^{-1}$and 1830 cm^{-1}or (F) 1728$cm^{-1}$and 1828 cm^{-1} respectively(Javaid et al 2019).

5.6 Degradative Analysis of PHA, PLA and PHA-PLA Blends

Bacterial degradation and environmental degradation analysis were conducted using thirteen samples of PHA (6), PLA (1) and PHA-PLA (6) blends with even surface and 0.1 g weight. Six PHA samples included PHA produced by strain PWA, PWC, PWF, PWG, DL3 and mixed culture on glucose, labelled as A, C, F, G, DL3 and M. Six PHA-PLA blends were labelled as PA, PC, PF, PG, PDL3 and PM for PHA sample of PWA, PWC, PWF, PWG, DL3 and mixed culture, respectively. All PHA and PHA-PLA films were prepared by solvent-cast technique. Polymer solution was poured in aluminum foil tray with the dimensions 1.0 cm x 1.0 cm. Films had 1.5 mm thickness and 0.1 g weight. In case of PLA, cast film was cut into small pieces having the dimensions 1.0 cm x 1.0 cm. PLA films had a thickness of 1.0 mm and weight of 0.1

grams. Only samples with even surface area were selected for studies. For each experiment to study degradation, all thirteen samples were prepared in triplicate. Before being used for experiments, samples were aged for 2 weeks.

5.6.1 Degradation in DifferentEnvironmental Systems

Degradation of PHA, PLA and PHA-PLA blends in different environmental systems i.e. soil, air, water, and heat were performed during start of September 2019 to end of January 2020 at the Department of Microbiology and Molecular Genetics, University of the Punjab.. In case of soil systems, samples were placed in wire mesh carefully and buried in a 20 inches deep hole dug at the base of *Syzygium cumini* (Jamun) tree. Study region was Study location was flat ground with brown coloration and smooth clay loam type soil. The average pH of soil was 4.5 and average temperature range during study was between 26℃ to 28℃. Soil microbial counts were 3.55 x 10^6, 3.58 x 10^6, 3.62 x 10^6, 3.65 x 10^6,and 3.70 x 10^6CFU/ml for 10^0 dilution during September to January. In case of air, samples were placed openly in test tubes at sites with maximum air distribution at MMG Research Lab II. Microbial counts in air were 2.52 x 10^2, 2.36 x 10^2, 2.47 x 10^2, 2.22 x 10^2, and 2.34 x 10^2 CFU/m^3 during September to January. Samples were placed at room temperature. In case of water, samples were placed in test tubes containing 10.0 ml untreated tap water having pH 8.2 and average temperature 25℃ and a microbial count of 208 CFU/ml. under semi-aerobic conditions. In case of heat, samples in test tubes were subjected to anaerobic degradation at constant temperature of 37℃ in an incubator.

5.6.2 Bacterial Degradation in Laboratory

Bacterial degradation was analyzed through a modified methodology combining two methods i.e. clear zone test (Nishida and Tokiwa 1993; Augusta et al 1993) and enzymatic degradation via mineralization (Tokiwa and Calabia 2004; Shah et al 2008; Ray and Kalia 2017b). Degradation of PHA, PLA and PHA-PLA blends by *Bacillus subtilis* and *Pseudomonas aeruginosa* were observed. N agar media (150.0 ml) was poured in 150 mm x 20 mm Pyrex® glass petri dishes. N agar plates were used to prepare lawn of bacterial culture. Samples were placed on N agar plates. Plates were incubated at 37℃ for 12 weeks.

5.6.3 Analysis of Samples During and After Degradation

For bacterial degradation, changes in sample morphology, sample color, changes in bacterial growth surrounding sample and changes in media surrounding sample were noted over a period of 12 weeks. For degradation in different environmental systems, changes in color and texture of samples were noted at regular intervals over a period of 20 weeks, as an indicator of degradation by physical appearance. Changes in fracture surfaces, crystallinity and overall microscopic degradation of samples was observed using light microscopy and scanning electron microscopy. Optical microscope, LABOMED, was used to observe sample degradation at 4X and 10X. Light micrographs were taken using IRMECO camera Scanning electron microscopy was conducted at 500 X, 1000 X, 2000 X and 3000 X magnification under low vacuum (80 Pa) using Zeiss EVO LS 10,operated at 20.0 kV acceleration voltage.Degradation by weight over 20 weeks was used as indication of sample biodegradation rate.For weight loss analysis, initial sample weight (W_i) was set at 0.1 grams as starting point. Each sample formulation was prepared in triplicate for all experiments. Samples were retrieved each week from sampling locations, rinsed with distilled

water and dried overnight. Constant weight was achieved by placing dried samples in a desiccator. Weight of each film was measured and recorded. Percentage weight change was calculated as follow:

$$Percentage\ Weight\ Change = \frac{(W_m - W_i)}{W_i}\ X\ 100$$

whereas W_i is the initial sample weight and $W_m$is the measured sample weight after degradation at regular intervals (Zhang and Thomas 2011; Ong and Sudesh 2016).

Differences in weight during degradation were analyzed by plotting weight (decigrams) against y axis and time (weeks) against x axis. Mean values recorded during triplicate experiments were used. Standard error and standard deviation for triplicate formulations of samples were calculated.

6 Declarations

6.1 Ethics approval and consent to participate

Not applicable

6.2 Consent for publication

Not applicable

6.3 Availability of data and materials

All data generated or analysed during this study are included in this published article.

6.4 Competing interests

The authors declare that they have no competing interest.

6.5 Funding

Not applicable

6.6 Authors' contributions

RS performed experiments and wrote manuscripts while NJ supervised, designed experiments and edited manuscript. All authors read and approved the final manuscript.

6.7 Acknowledgements

Not applicable

6.8 Authors' information

Not applicable

7 References

Aljuraifani AA, Berekaa MM, Ghazwani AA (2019) Bacterial biopolymer (polyhydroxyalkanoate) production from low-cost sustainable sources. MicrobiologyOpen 8(6):e00755

Augusta J, Müller R-J, Widdecke H (1993) A rapid evaluation plate-test for the biodegradability of plastics. Appl Microbiol Biotechnol 39(4-5):673-678

Ausejo JG, Rydz J, Musioł M et al (2018) A comparative study of three-dimensional printing directions: The degradation and toxicological profile of a PLA/PHA blend. Polym Degradation Stab 152:191-207

641 Basnet S, Wiberg B (2016) Production of Polylactic acid in laboratory scale, and characterising
642 the thermal properties. Degree thesis, Arcada University of Technology.
643 Chaudhry WN, Jamil N, Ali I et al (2011) Screening for polyhydroxyalkanoate (PHA)-producing
644 bacterial strains and comparison of PHA production from various inexpensive carbon sources.
645 Ann Microbiol 61(3):623-629
646 EstructuraProteinas (2020) Bioplastic from starch - home made.
647 https://www.youtube.com/watch?v=y1joh_t1thc&t=19s. Accessed 29 Jan 2020
648 Fossi MC, Vlachogianni T, Galgani F et al (2020) Assessing and mitigating the harmful effects
649 of plastic pollution: the collective multi-stakeholder driven Euro-Mediterranean response. Ocean
650 Coast Manage 184(2020):105005
651 Gopi S, Kontopoulou M, Ramsay BA et al (2018) Manipulating the structure of medium-chain-
652 length polyhydroxyalkanoate (MCL-PHA) to enhance thermal properties and crystallization
653 kinetics. Int J Biol Macromol 119(2018):1248-1255. doi:10.1016/j.ijbiomac.2018.08.016
654 Green Plastics (2012) The new science of bioplastic. Green-plastics.net website: https://green-
655 plastics.net/ Accessed 29 Jan 2020
656 Ismail NA, Mohd Tahir S, Yahya N et al (2016) Synthesis and characterization of biodegradable
657 starch-based bioplastics. In: Mater Sci Forum. Trans Tech Publ, p 673-678
658 Iwata T (2015) Biodegradable and bio-based polymers: future prospects of eco-friendly plastics.
659 Angew Chem Int Ed 54(11):3210-3215
660 Javaid N, Batool R, Jamil N (2019) Blend of Polyhydroxyalkanoates Synthesized By Lipase
661 Positive Bacteria From Plant Oils. Journal of Renewable Materials 7(5):460-473

662 Johnston B, Jiang G, Hill D et al (2017) The molecular level characterization of biodegradable
663 polymers originated from polyethylene using non-oxygenated polyethylene wax as a carbon
664 source for polyhydroxyalkanoate production. Bioengineering 4(3):73
665 Karaffa LS (2013) The Merck index: an encyclopedia of chemicals, drugs, and biologicals. RSC
666 Publishing.
667 Keziah VS, Gayathri R, Priya VV (2018) Biodegradable plastic production from corn starch.
668 Drug Invent Today 10(7):1315-1317
669 Kirchnerová J, Cave GC (1976) The solubility of water in low-dielectric solvents. Can J Chem
670 54(24):3909-3916
671 Koller M (2018) Biodegradable and Biocompatible Polyhydroxy-alkanoates (PHA): Auspicious
672 Microbial Macromolecules for Pharmaceutical and Therapeutic Applications. Molecules
673 23(2):362. doi:10.3390/molecules23020362
674 Koller M, Dias MMdS, Rodríguez-Contreras A et al (2015) Liquefied wood as inexpensive
675 precursor-feedstock for bio-mediated incorporation of (R)-3-hydroxyvalerate into
676 polyhydroxyalkanoates. Materials 8(9):6543-6557
677 Kricheldorf HR (2001) Syntheses and application of polylactides. Chemosphere 43(1):49-54.
678 doi:10.1016/s0045-6535(00)00323-4
679 La Mantia F, Morreale M, Botta L et al (2017) Degradation of polymer blends: A brief review.
680 Polym Degradation Stab 145:79-92
681 Leja K, Lewandowicz G (2010) Polymer Biodegradation and Biodegradable Polymers-a Review.
682 Pol J Environ Stud 19(2):255-266
683 Li Z, Loh XJ (2015) Water soluble polyhydroxyalkanoates: future materials for therapeutic
684 applications. Chem Soc Rev 44(10):2865-2879. doi:10.1039/c5cs00089k

685 Li Z, Yang J, Loh XJ (2016) Polyhydroxyalkanoates: opening doors for a sustainable future.
686 NPG Asia Mater 8(4):e265
687 Mackay D, Bobra A, Shiu W et al (1980) Relationships between aqueous solubility and octanol-
688 water partition coefficients. Chemosphere 9(11):701-711
689 Marichelvam M, Jawaid M, Asim M (2019) Corn and rice starch-based bio-plastics as alternative
690 packaging materials. Fibers 7(4):32
691 Masood F, Abdul-Salam M, Yasin T et al (2017) Effect of glucose and olive oil as potential
692 carbon sources on production of PHAs copolymer and tercopolymer by Bacillus cereus FA11. 3
693 Biotech 7(1):87
694 Modjarrad K, Ebnesajjad S (2013) Handbook of polymer applications in medicine and medical
695 devices. Elsevier.
696 Mondal R (2015) Synthesis and characterization of Starch based biocomposite films and their
697 degradation behavior--an alternative to the conventional polymer. Doctoral dissertation, National
698 institute of technology, Rourkela.
699 Msuya N, Katima J, Massanja E et al (2017) Poly (lactic-acid) Production-from Monomer to
700 Polymer: A review. J Polym Sci 1(1):
701 Muller J, González-Martínez C, Chiralt A (2017) Combination of poly (lactic) acid and starch for
702 biodegradable food packaging. Materials 10(8):952
703 Munir S, Jamil N (2018) Polyhydroxyalkanoates (PHA) production in bacterial co-culture using
704 glucose and volatile fatty acids as carbon source. J Basic Microbiol 58(3):247-254
705 Muniyasamy S, Muniyasamy S, Mohanrasu K et al (2019) Biobased Biodegradable Polymers for
706 Ecological Applications: A Move Towards Manufacturing Sustainable Biodegradable Plastic
707 Products. Integrating Green Chemistry & Sustainable Engineering.

708 Muthuraj R, Misra M, Mohanty AK (2018) Biodegradable compatibilized polymer blends for
709 packaging applications: A literature review. J Appl Polym Sci 135(24):45726
710 Narancic T, Verstichel S, Reddy Chaganti S et al (2018) Biodegradable plastic blends create new
711 possibilities for end-of-life management of plastics but they are not a panacea for plastic
712 pollution. Environ Sci Technol 52(18):10441-10452
713 Nerkar M, Ramsay JA, Ramsay BA et al (2015) Improvements in the melt and solid-state
714 properties of poly (lactic acid), poly-3-hydroxyoctanoate and their blends through reactive
715 modification. Polym Plast Technol Eng 64:51-61
716 Nishida H, Tokiwa Y (1993) Distribution of poly (β-hydroxybutyrate) and poly (ε-caprolactone)
717 aerobic degrading microorganisms in different environments. J Environ Polym Degrad 1(3):227-
718 233
719 Ong SY, Sudesh K (2016) Effects of polyhydroxyalkanoate degradation on soil microbial
720 community. Polym Degradation Stab 131:9-19
721 Pretula J, Slomkowski S, Penczek S (2016) Polylactides—Methods of synthesis and
722 characterization. Adv Drug Deliv Rev 107(2016):3-16
723 Radecka I, Irorere V, Jiang G et al (2016) Oxidized polyethylene wax as a potential carbon
724 source for PHA production. Materials 9(5):367
725 Rasal RM, Bohannon BG, Hirt DE (2008) Effect of the photoreaction solvent on surface and
726 bulk properties of poly(lactic acid) and poly(hydroxyalkanoate) films. J Biomed Mater Res B
727 Appl Biomater 85(2):564-572. doi:10.1002/jbm.b.30980
728 Ray S, Kalia VC (2017a) Biological significance of degradation of polyhydroxyalkanoates. In:
729 Microbial Applications, vol 1. Springer, Cham, p 125-139. doi:https://doi.org/10.1007/978-3-
730 319-52666-9_5

731 Ray S, Kalia VC (2017b) Polyhydroxyalkanoate Production and Degradation Patterns in Bacillus
732 Species. Indian J Microbiol 57(4):387-392. doi:10.1007/s12088-017-0676-y
733 Reddy C, Ghai R, Kalia VC (2003) Polyhydroxyalkanoates: an overview. Bioresour Technol
734 87(2):137-146
735 Rehman S, Jamil N, Husnain S (2007) Screening of different contaminated environments for
736 polyhydroxyalkanoates-producing bacterial strains. Biologia 62(6):650-656
737 Roy I, Visakh P (2014) Polyhydroxyalkanoate (PHA) based blends, composites and
738 nanocomposites, Vol 30. Royal Society of Chemistry.
739 Royte E (2006) Corn plastic to the rescue. Smithsonian Magazine 37(5):84-88.
740 https://www.smithsonianmag.com/science-nature/corn-plastic-to-the-rescue-126404720/
741 Rudnik E (2019) Compostable polymer materials. Second edn. Elsevier.
742 Sarasa J, Gracia JM, Javierre C (2009) Study of the biodisintegration of a bioplastic material
743 waste. Bioresour Technol 100(15):3764-3768. doi:10.1016/j.biortech.2008.11.049
744 Shah AA, Hasan F, Hameed A et al (2008) Biological degradation of plastics: a comprehensive
745 review. Biotechnol Adv 26(3):246-265. doi:10.1016/j.biotechadv.2007.12.005
746 Shah TV, Vasava DV (2019) A glimpse of biodegradable polymers and their biomedical
747 applications. epoly 19(1):385-410
748 Shogren R (2009) Starch-poly (hydroxyalkanoate) composites and blends. Biodegrad Polym
749 Blends Compos from Renew Resour, John Wiley & Sons, Inc:211-226
750 Sintim HY, Bary AI, Hayes DG et al (2019) Release of micro- and nanoparticles from
751 biodegradable plastic during in situ composting. Sci Total Environ 675:686-693.
752 doi:10.1016/j.scitotenv.2019.04.179

753 Sohail R, Jamil N (2019) Isolation of biosurfactant producing bacteria from Potwar oil fields:
754 Effect of non-fossil fuel based carbon sources. Green Process Synth 9(1):77-86
755 Sohail R, Jamil N, Ali I et al (2020) Animal fat and glycerol bioconversion to
756 polyhydroxyalkanoate by produced water bacteria. epoly 20(1):92-102
757 Solomonides EG (2016) Biodegradable bioplastic compositions and methods of making and
758 using the same.
759 Su S, Kopitzky R, Tolga S et al (2019) Polylactide (PLA) and Its Blends with Poly(butylene
760 succinate) (PBS): A Brief Review. Polymers (Basel) 11(7):1193. doi:10.3390/polym11071193
761 Tan G-YA, Chen C-L, Li L et al (2014) Start a research on biopolymer polyhydroxyalkanoate
762 (PHA): a review. Polymers 6(3):706-754
763 Teeka J, Imai T, Cheng X et al (2010) Screening of PHA-producing bacteria using biodiesel-
764 derived waste glycerol as a sole carbon source. J Water Environ Technol 8(4):373-381
765 Tokiwa Y, Calabia BP (2004) Review degradation of microbial polyesters. Biotechnol Lett
766 26(15):1181-1189
767 Van Doan T, Hoi LT, Phong TH (2015) Recovery of Poly (3-hydroxybutyrate) from Yangia sp.
768 ND199 by Simple Digestion with sodium hypochlorite. Vietnam Journal of Science and
769 Technology 53(6):706
770 Verma R, Vinoda K, Papireddy M et al (2016) Toxic pollutants from plastic waste-a review.
771 Procedia Environ Sci 35:701-708
772 Volova T, Boyandin A, Vasiliev A et al (2010) Biodegradation of polyhydroxyalkanoates
773 (PHAs) in tropical coastal waters and identification of PHA-degrading bacteria. Polym
774 Degradation Stab 95(12):2350-2359

775 Yang S (2014) Novel bio-based and biodegradable polymer blends. Dissertation Thesis, Iowa
776 State University.
777 Zerbi G, Gallino G, Del Fanti N et al (1989) Structural depth profiling in polyethylene films by
778 multiple internal reflection infra-red spectroscopy. Polym Plast Technol Eng 30(12):2324-2327
779 Zhang J, Yan D-X, Xu J-Z et al (2012) Highly crystallized poly (lactic acid) under high pressure.
780 AIP Advances 2(4):042159
781 Zhang M, Thomas NL (2011) Blending polylactic acid with polyhydroxybutyrate: the effect on
782 thermal, mechanical, and biodegradation properties. Adv Polym Tech 30(2):67-79
783 Zinn M, Witholt B, Egli T (2001) Occurrence, synthesis and medical application of bacterial
784 polyhydroxyalkanoate. Adv Drug Deliv Rev 53(1):5-21. doi:10.1016/s0169-409x(01)00218-6

785

8 Figure Titles

Figure 1 FT-IR Spectrum of PHA Sample of Strain PWF

Figure 2 FT-IR Spectrum of PHA Sample of Mixed Culture

Figure 3 FT-IR Spectrum of PLA Sample.

Figure 4 FT-IR Spectrum of PHA-PLA Sample of Strain PWF

Figure 5 FT-IR Spectrum of PHA-PLA Sample of Mixed Culture

Figure 6 SEM of PHA sample F (A), PLA (B) and PHA-PLA sample PF (C) before and after degradation at 3000 X.

Figure 7 Graphical representation for soil degradation of PHA, PLA, and PHA-PLA blends.

Figure 8 Graphical representation for water degradation of PHA, PLA, and PHA-PLA blends.

Figure 9 Graphical representation for air degradation of PHA, PLA, and PHA-PLA blends.

Figure 10 Graphical representation for heat degradation of PHA, PLA, and PHA-PLA blends.

9 Table Titles

Table 1PHA Production on Glucose

Figures

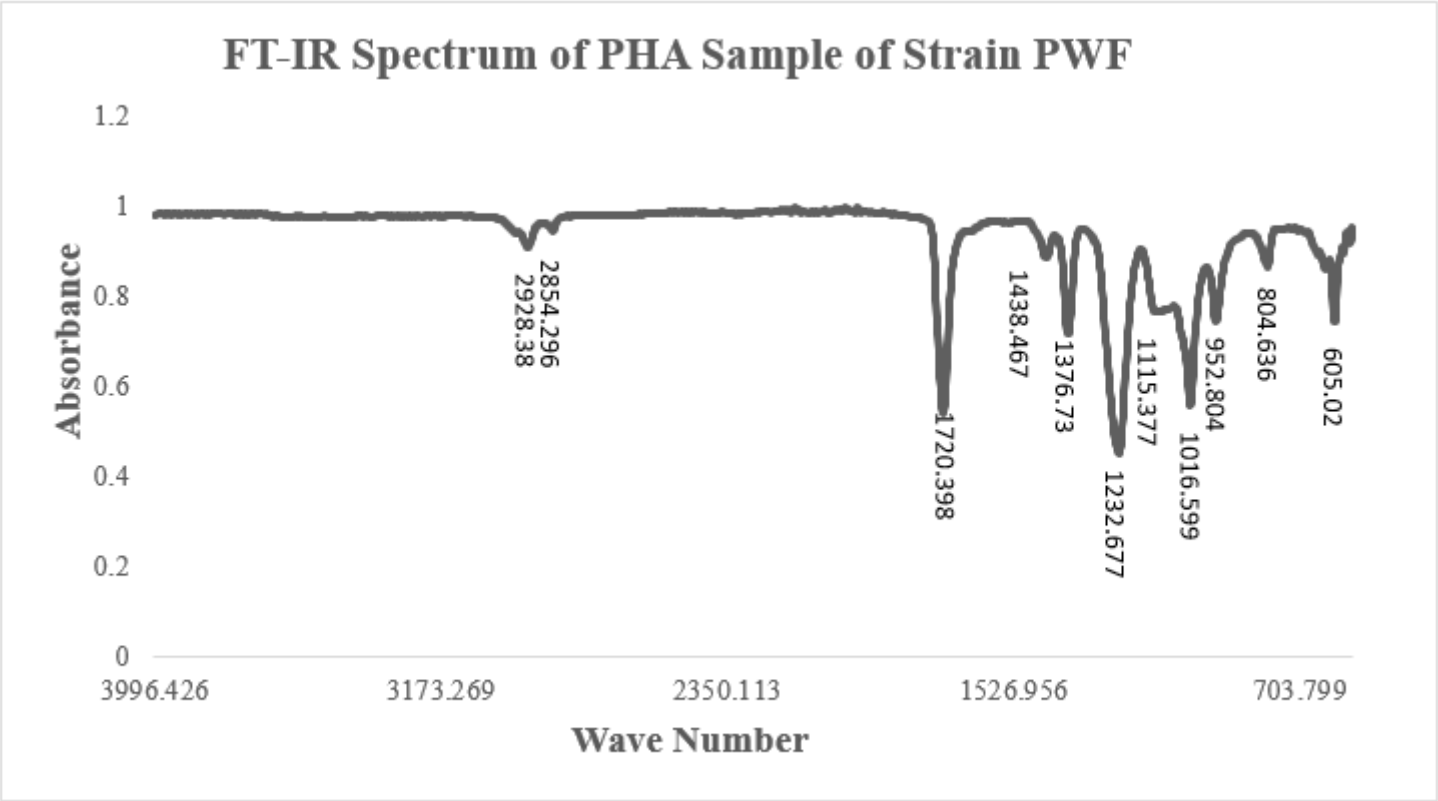

Figure 1

FT-IR Spectrum of PHA Sample of Strain PWF

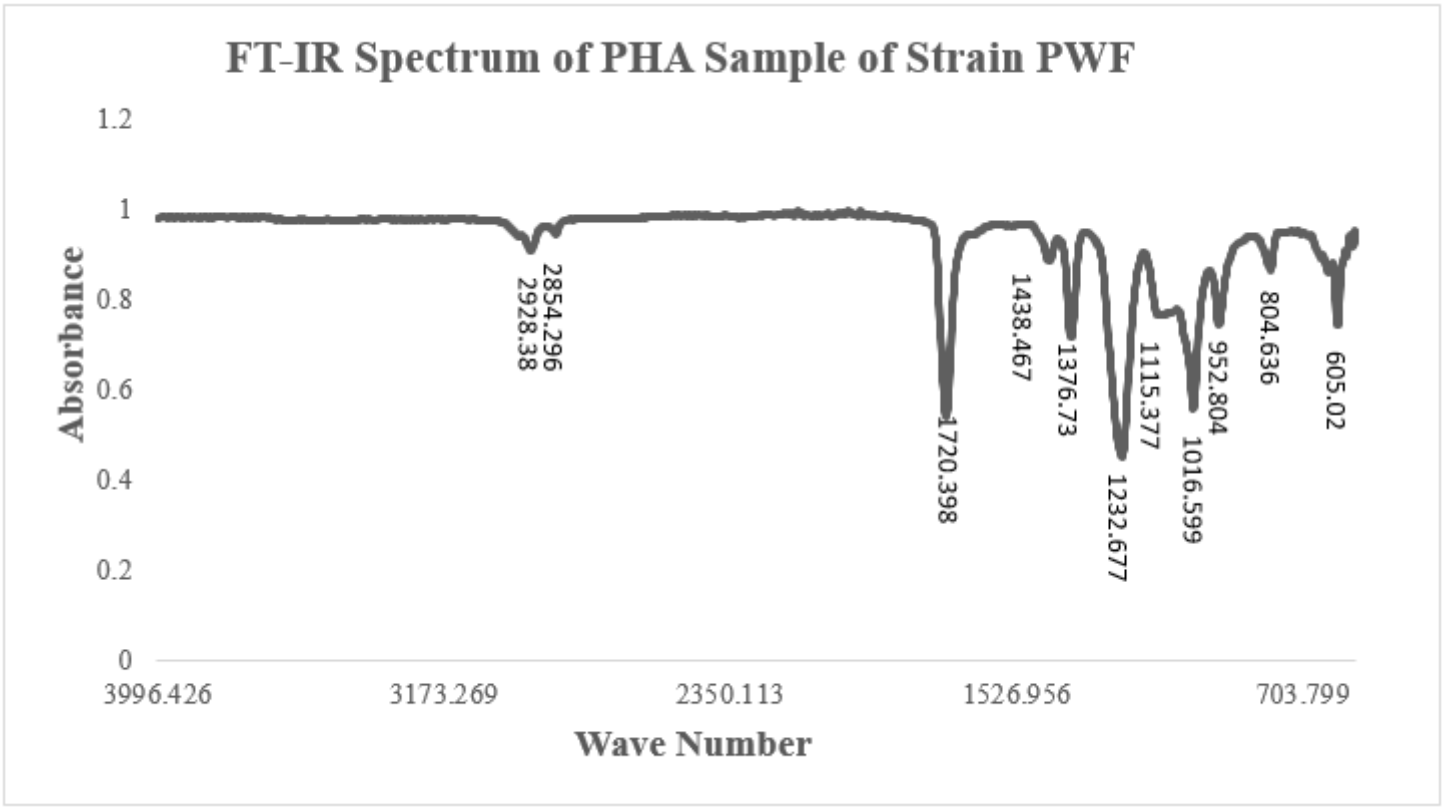

Figure 1

FT-IR Spectrum of PHA Sample of Strain PWF

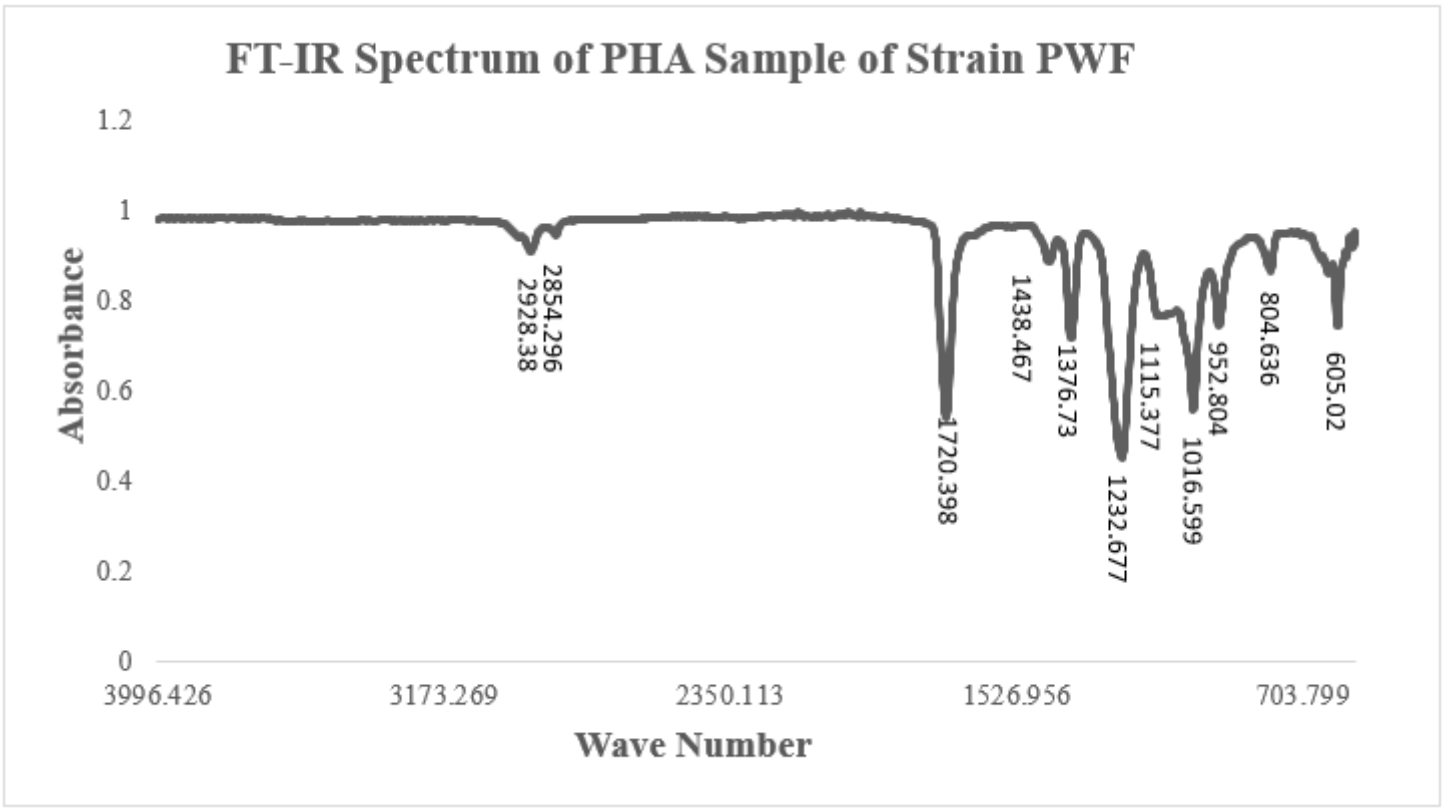

Figure 1

FT-IR Spectrum of PHA Sample of Strain PWF

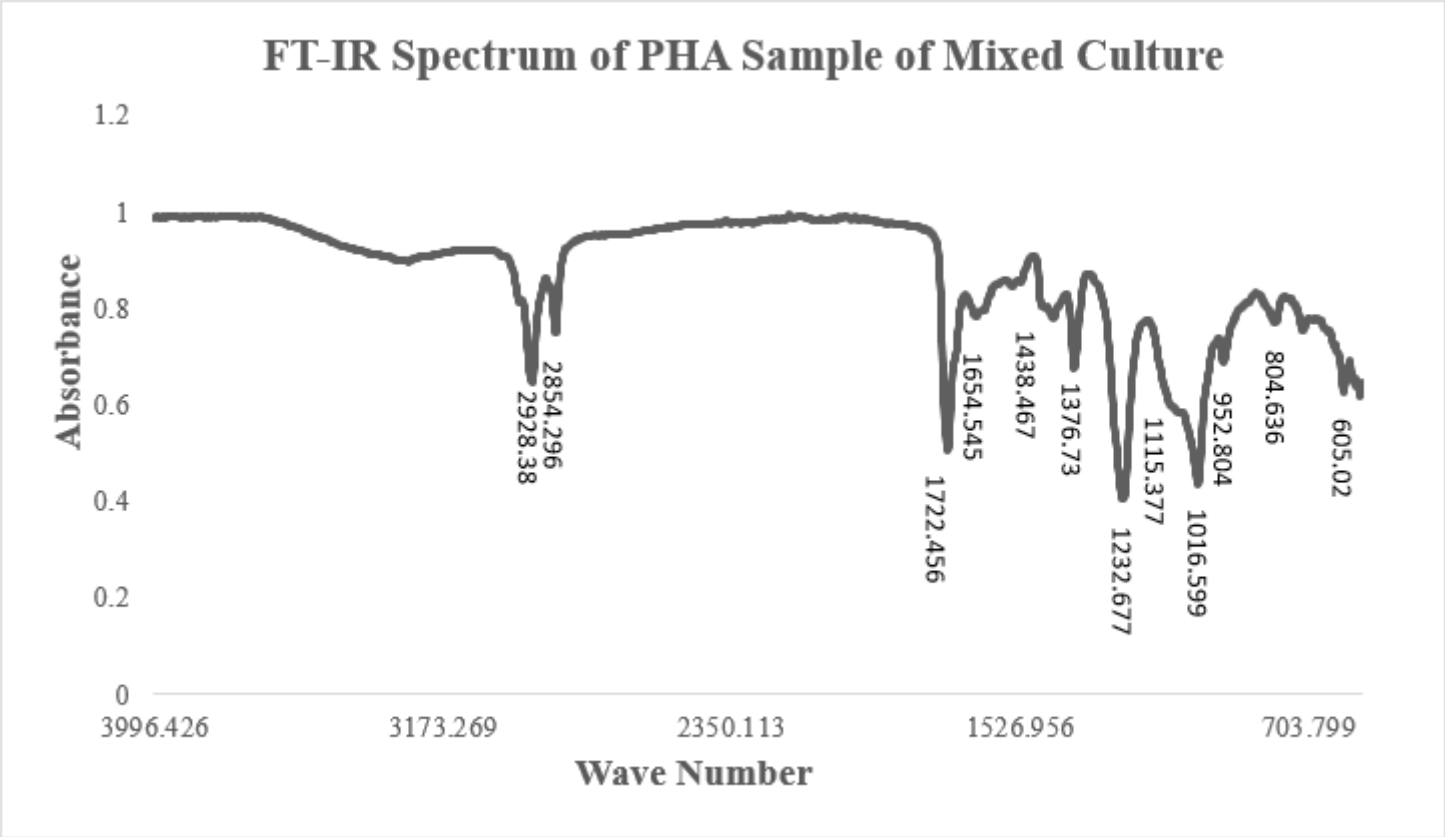

Figure 2

FT-IR Spectrum of PHA Sample of Mixed Culture

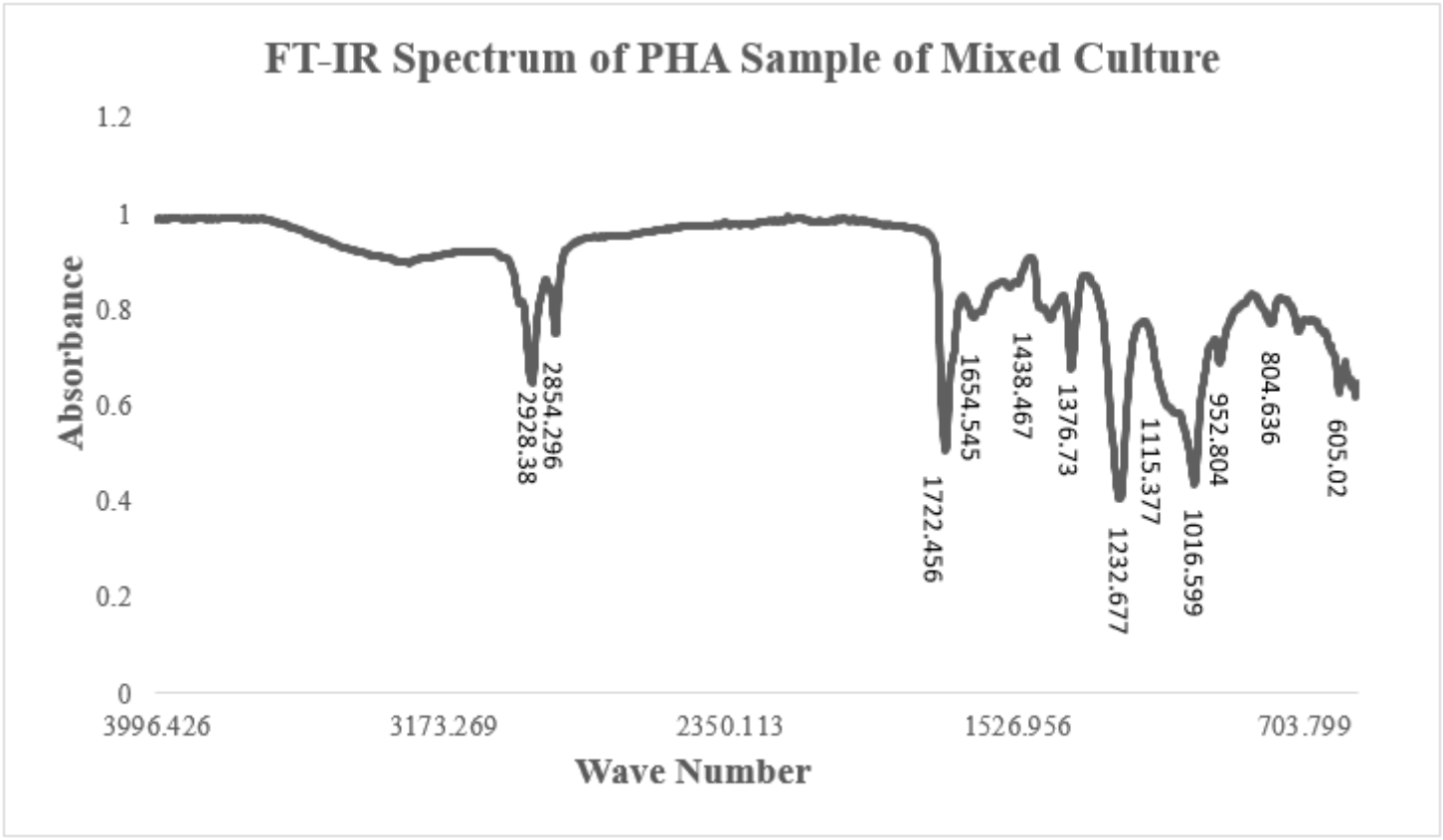

Figure 2

FT-IR Spectrum of PHA Sample of Mixed Culture

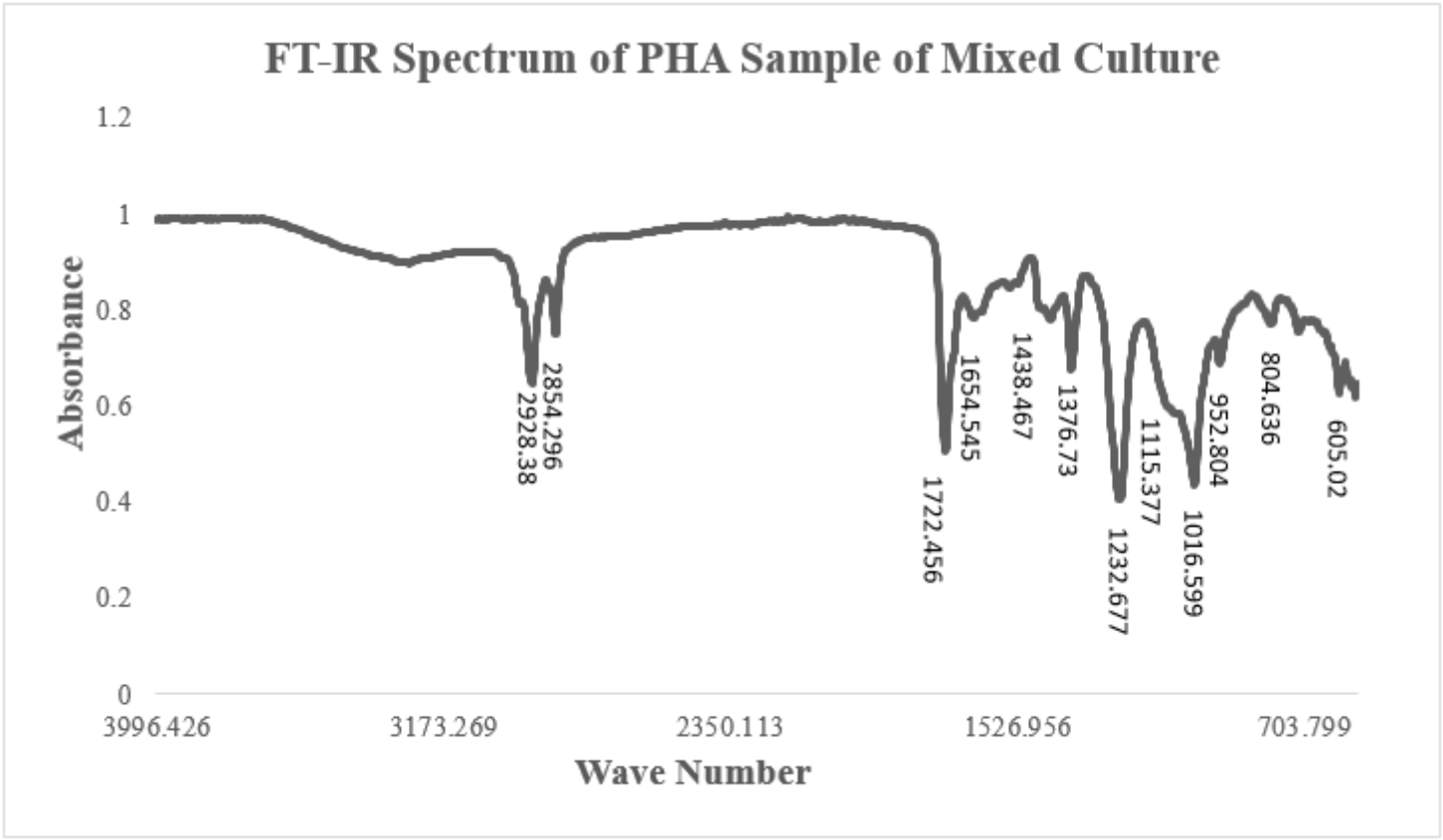

Figure 2

FT-IR Spectrum of PHA Sample of Mixed Culture

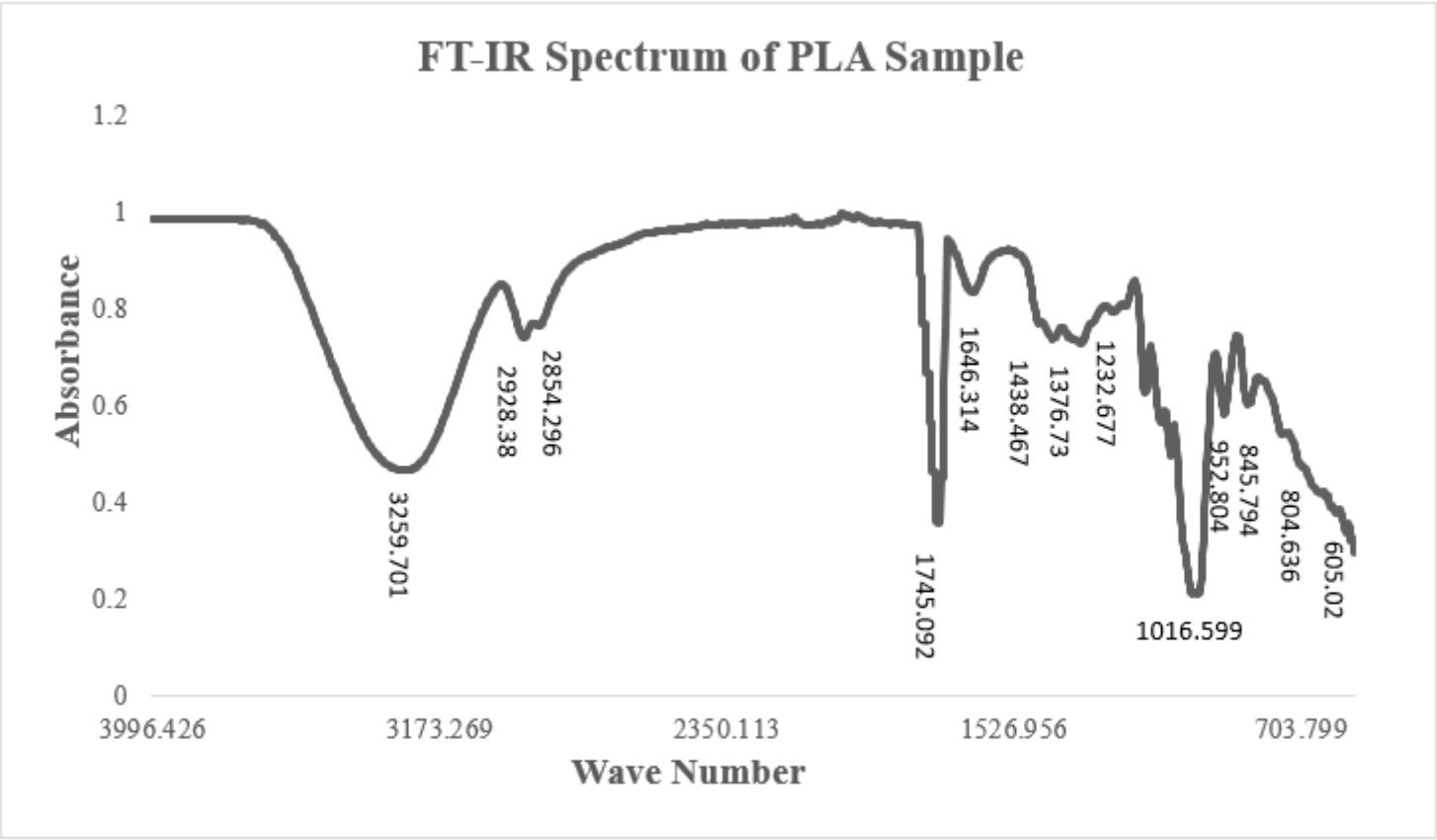

Figure 3

FT-IR Spectrum of PLA Sample.

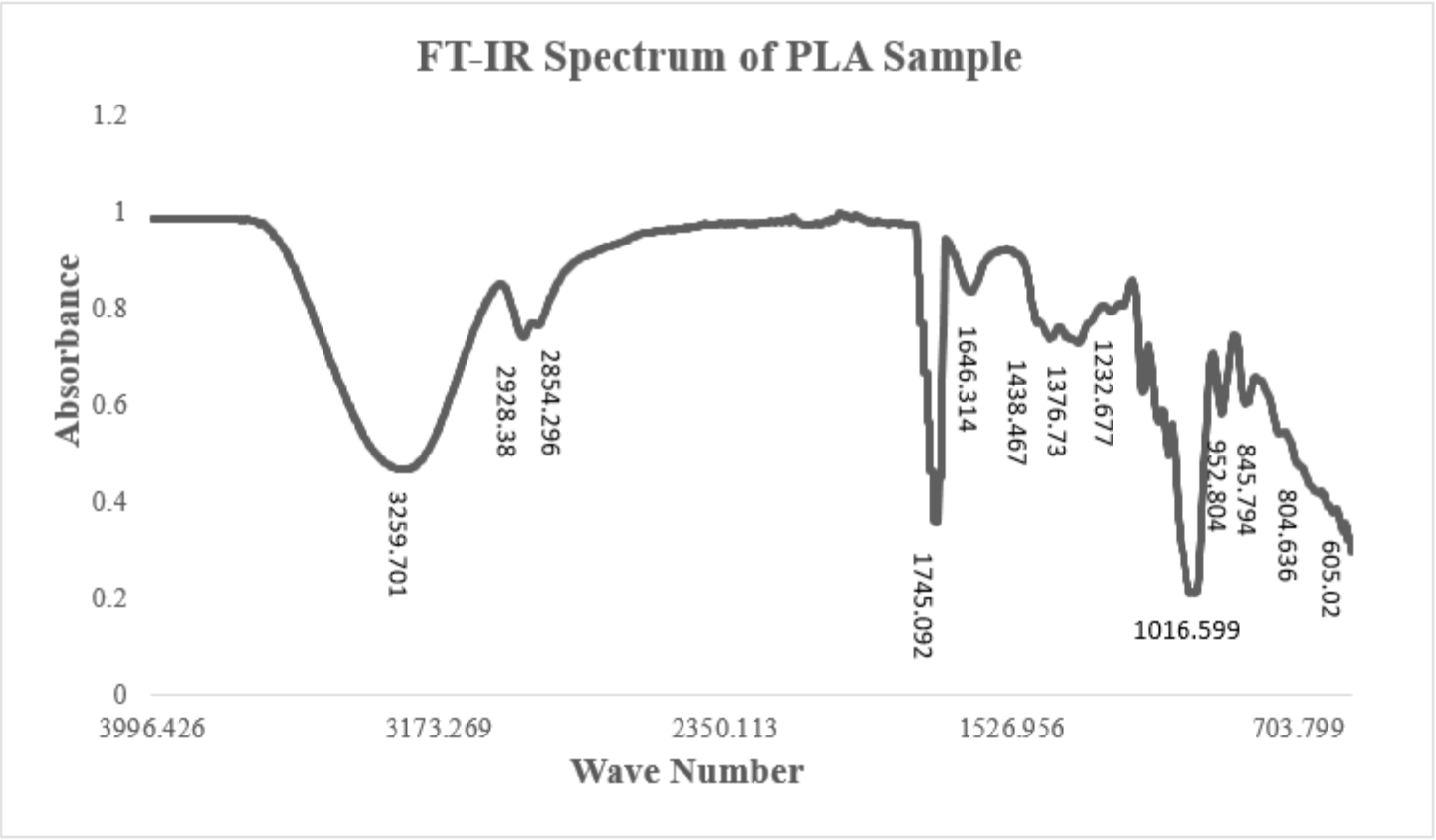

Figure 3

FT-IR Spectrum of PLA Sample.

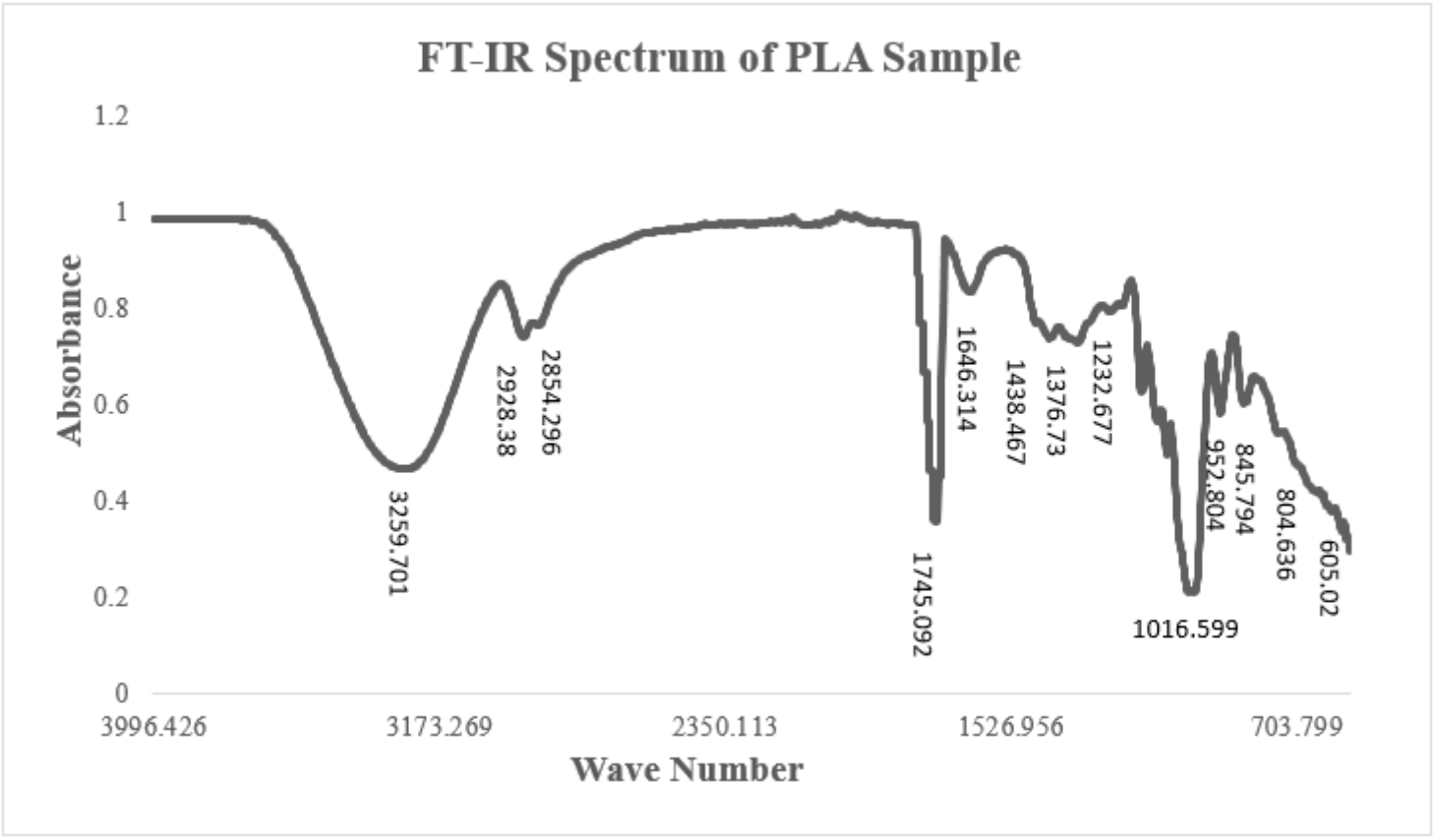

Figure 3

FT-IR Spectrum of PLA Sample.

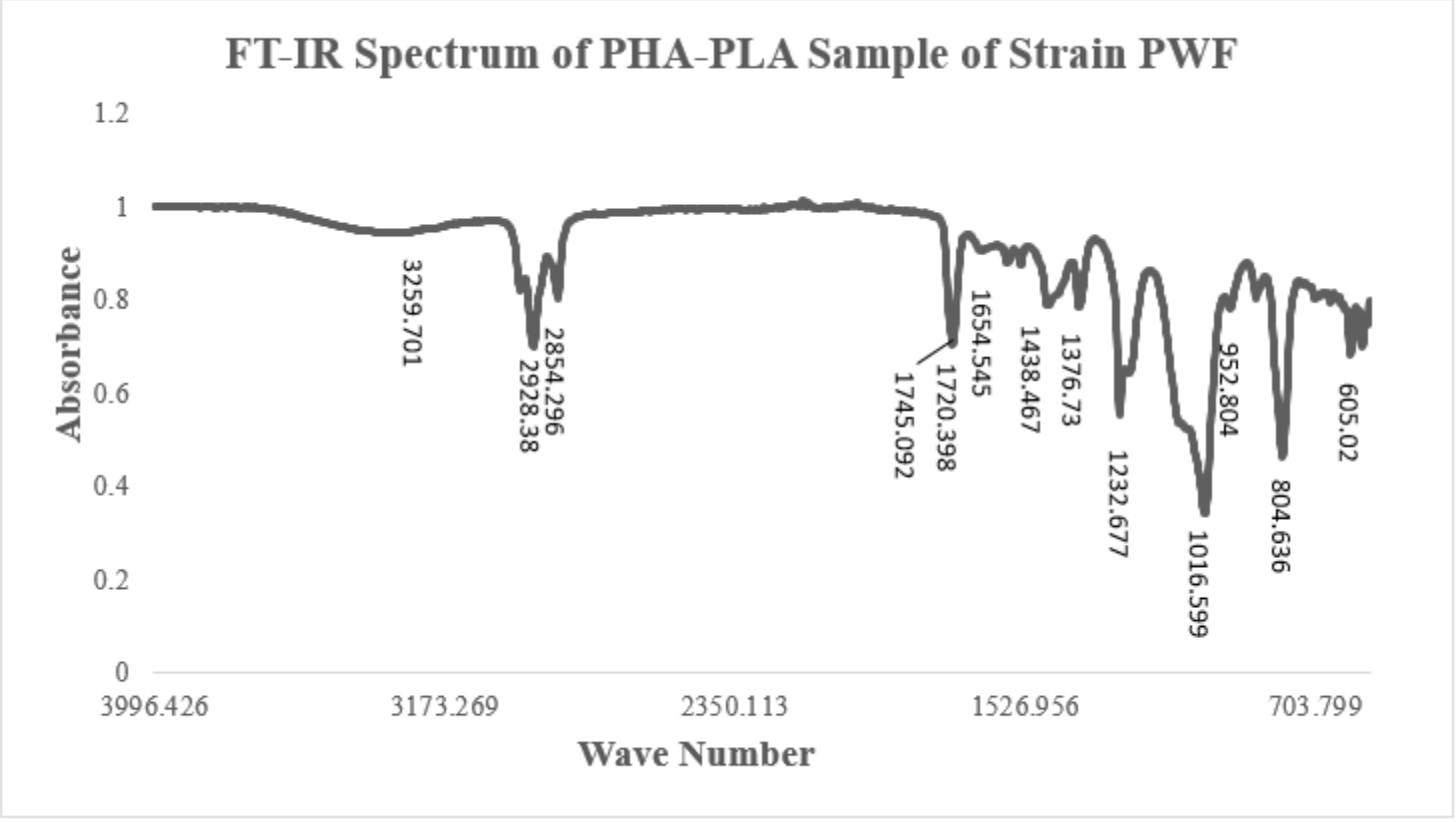

Figure 4

FT-IR Spectrum of PHA-PLA Sample of Strain PWF

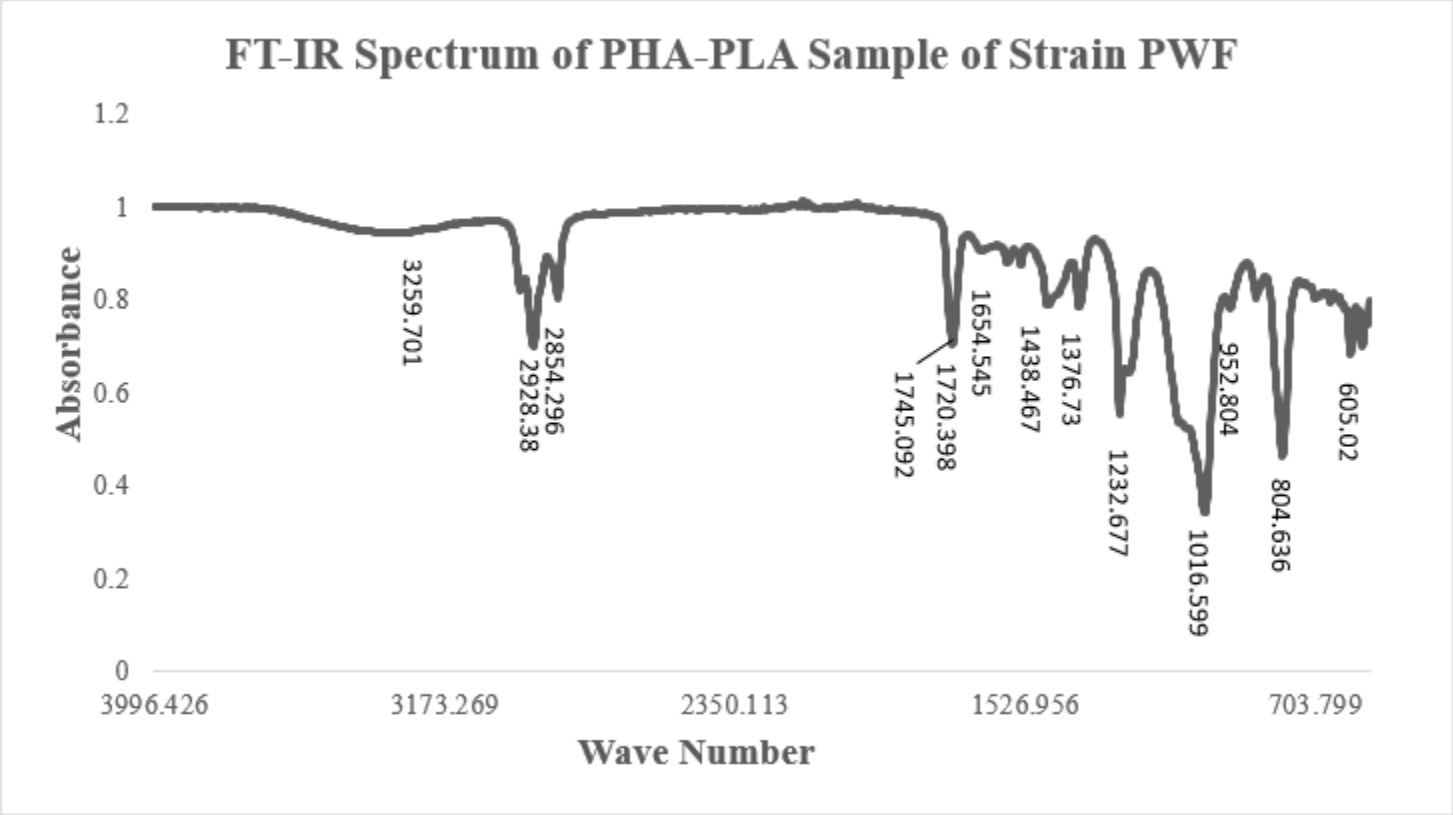

Figure 4

FT-IR Spectrum of PHA-PLA Sample of Strain PWF

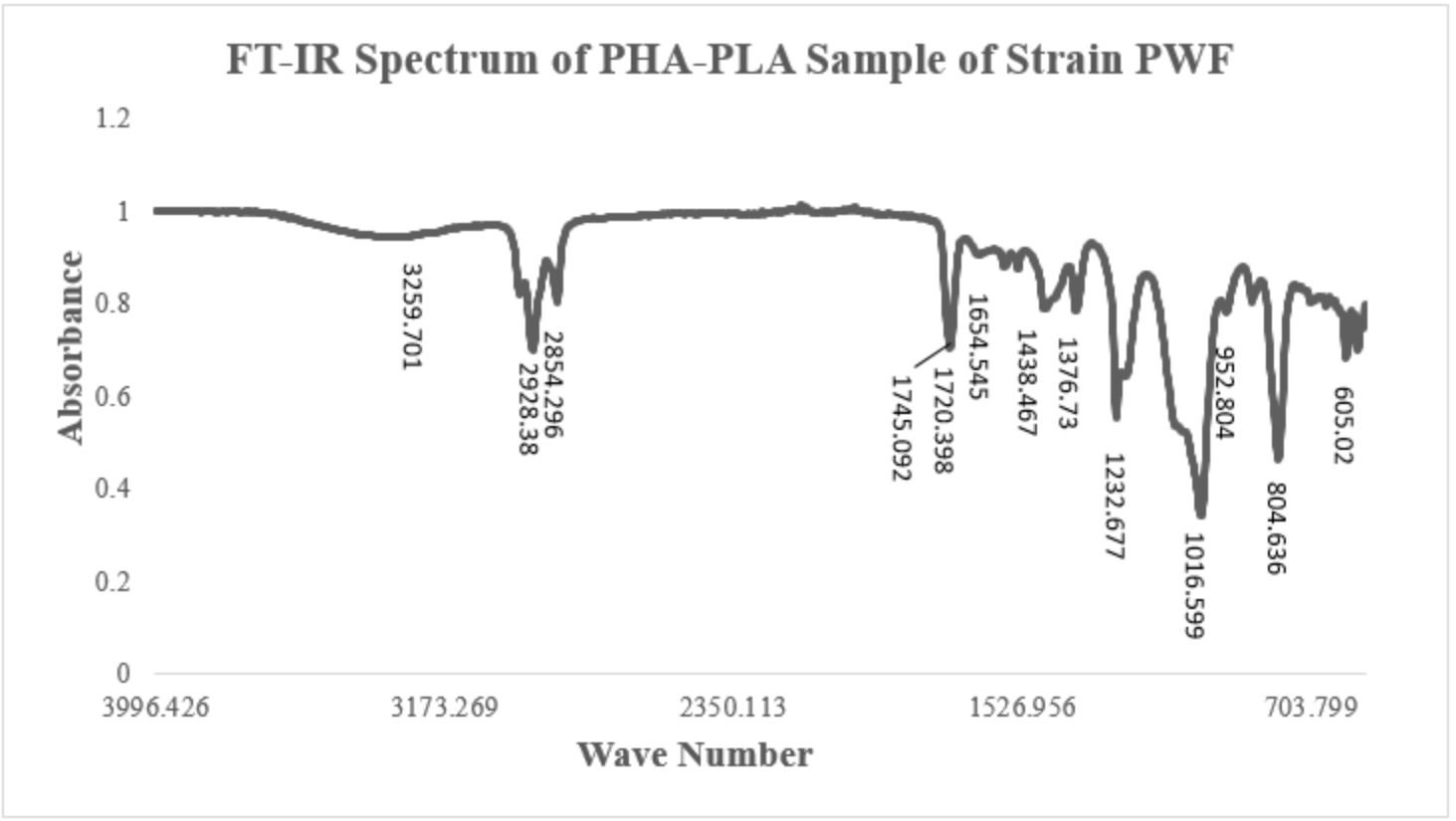

Figure 4

FT-IR Spectrum of PHA-PLA Sample of Strain PWF

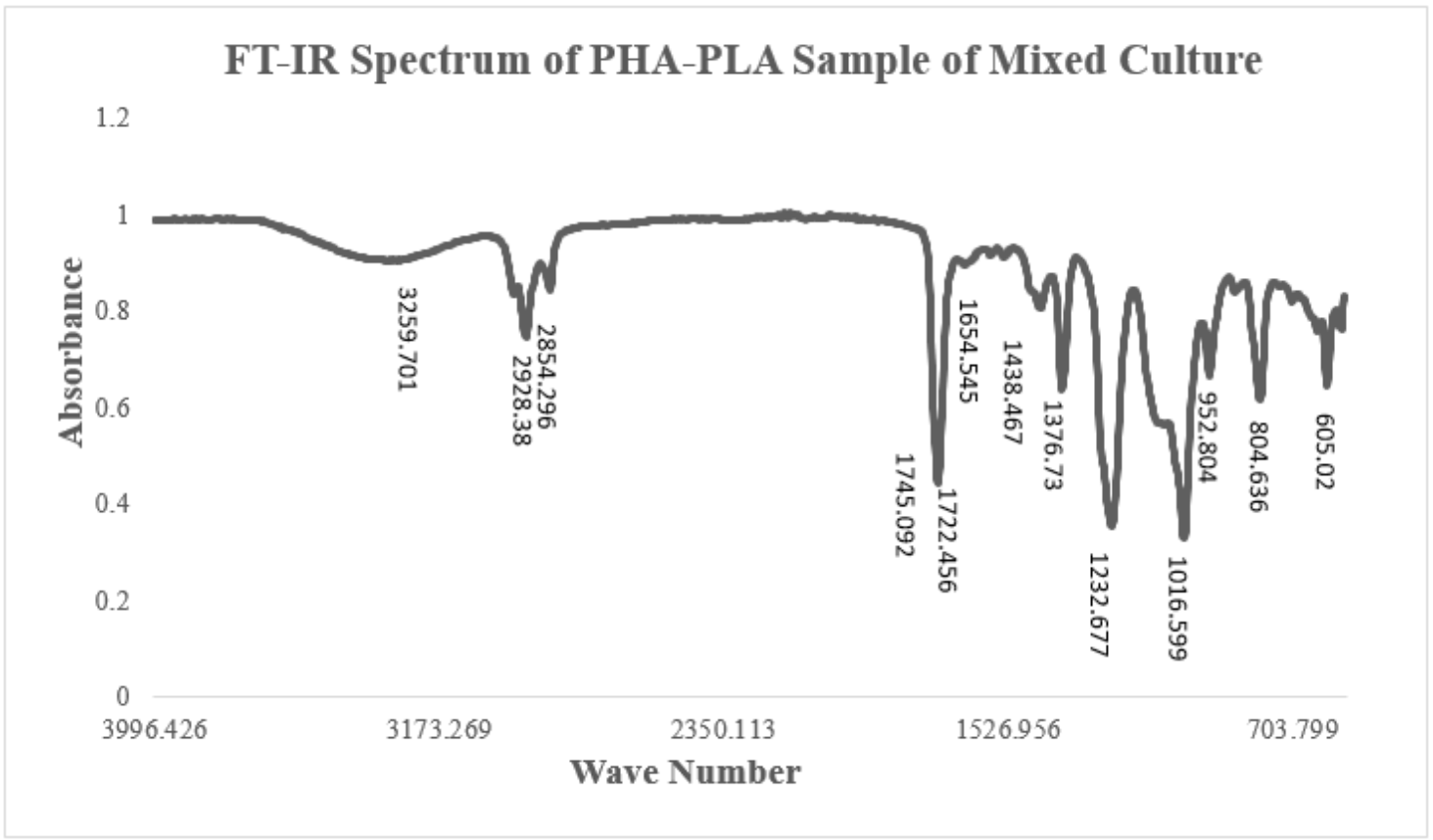

Figure 5

FT-IR Spectrum of PHA-PLA Sample of Mixed Culture

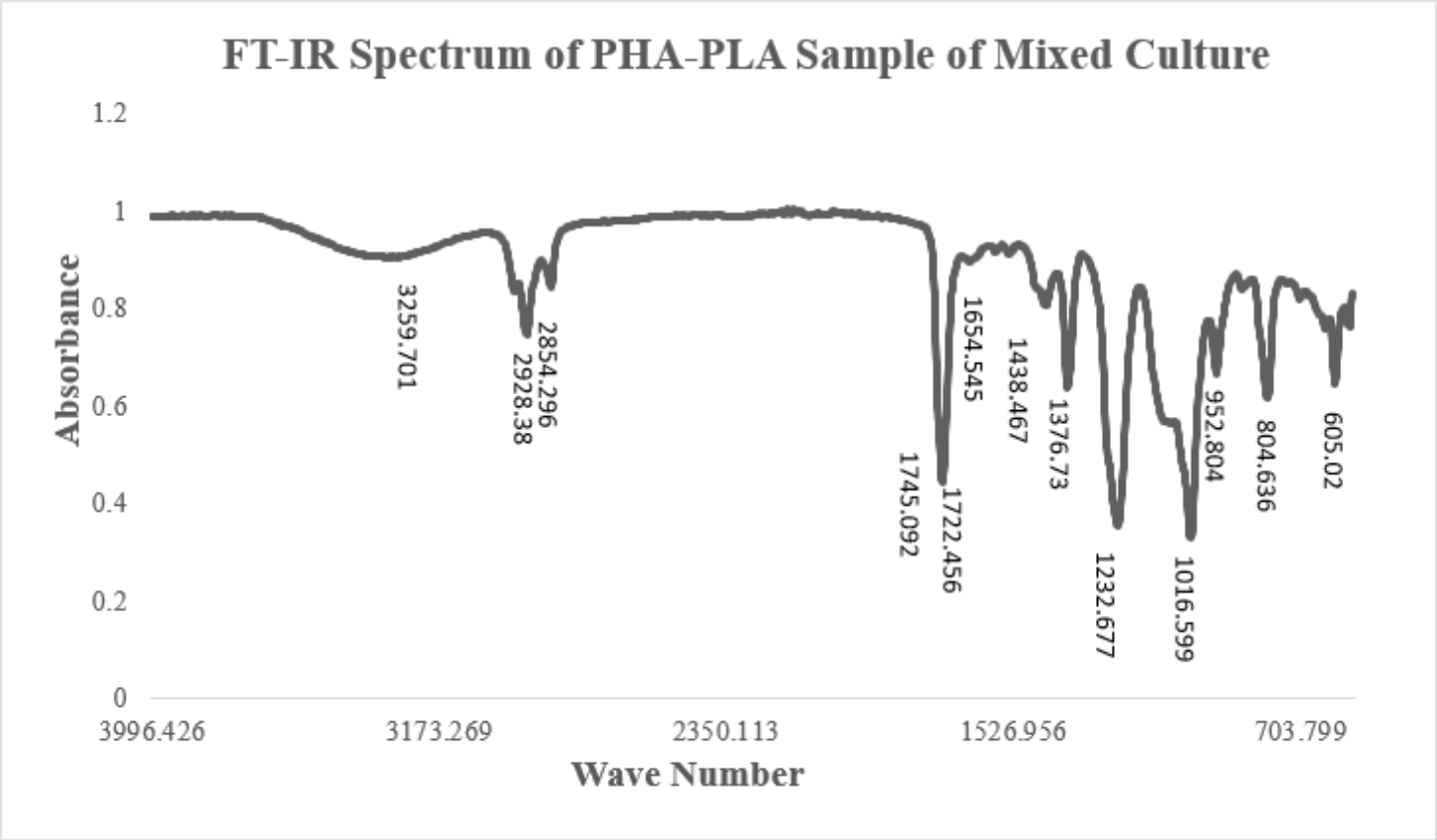

Figure 5

FT-IR Spectrum of PHA-PLA Sample of Mixed Culture

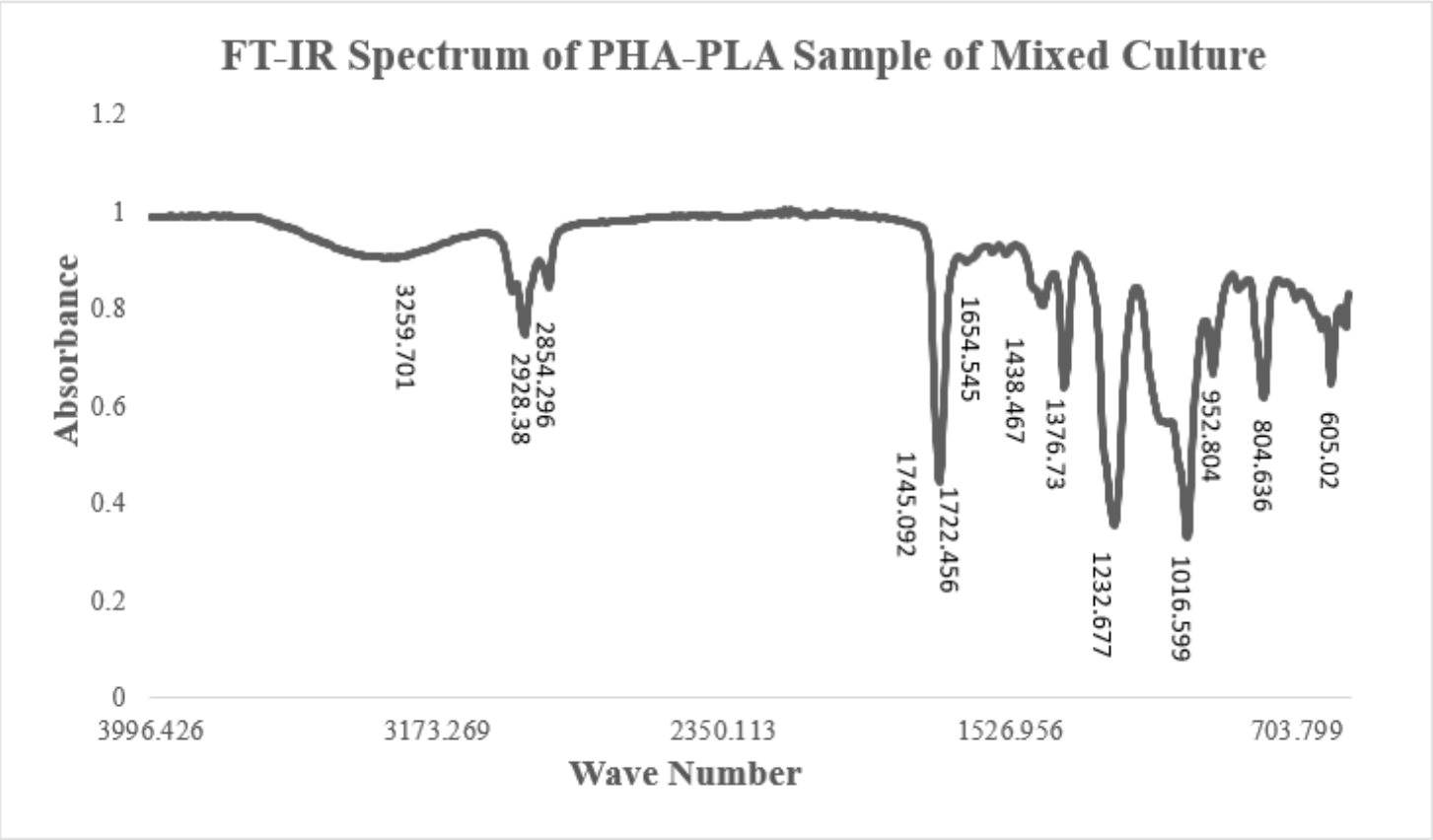

Figure 5

FT-IR Spectrum of PHA-PLA Sample of Mixed Culture

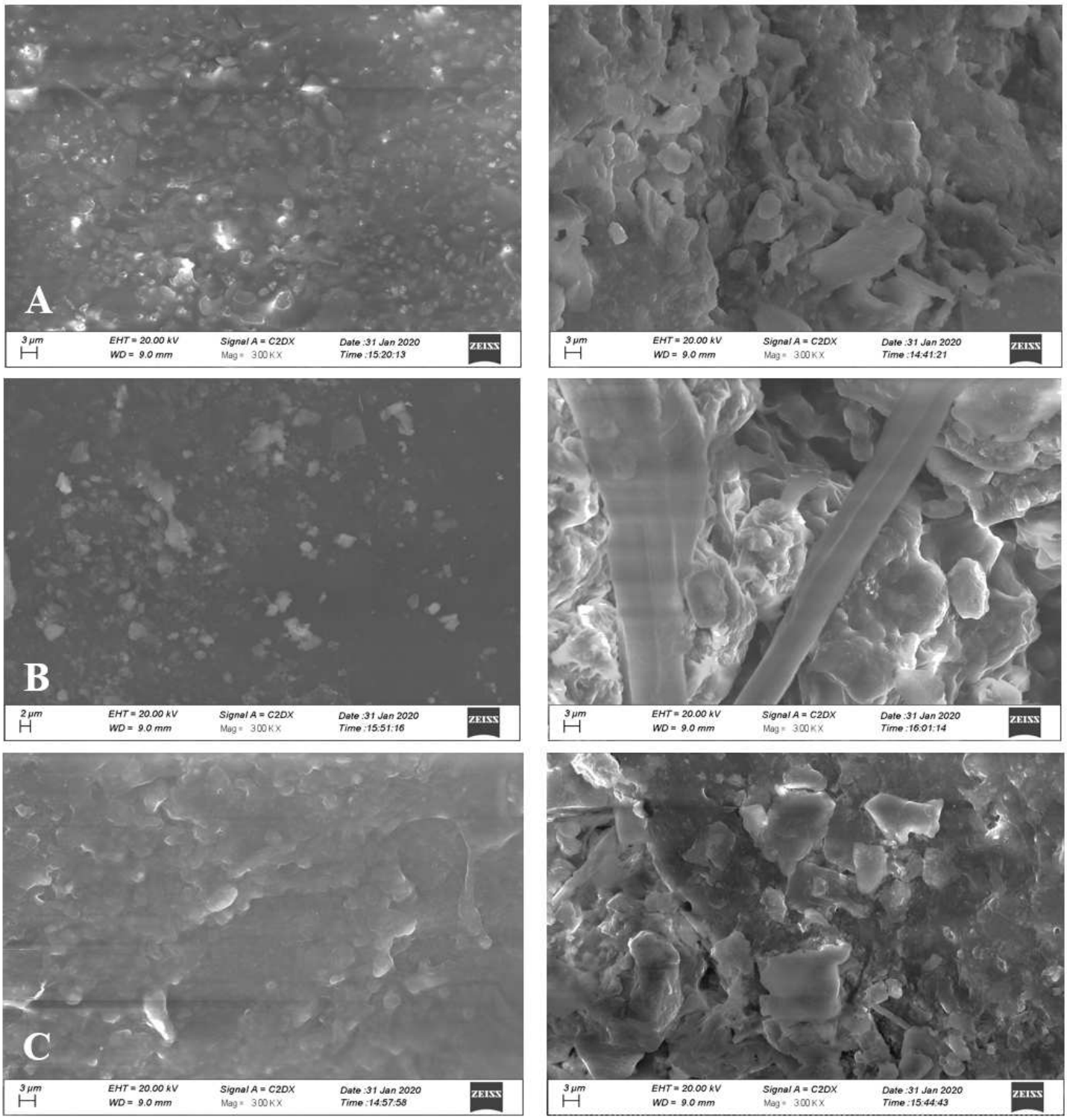

Figure 6

SEM of PHA sample F (A), PLA (B) and PHA-PLA sample PF (C) before and after degradation at 3000 X.

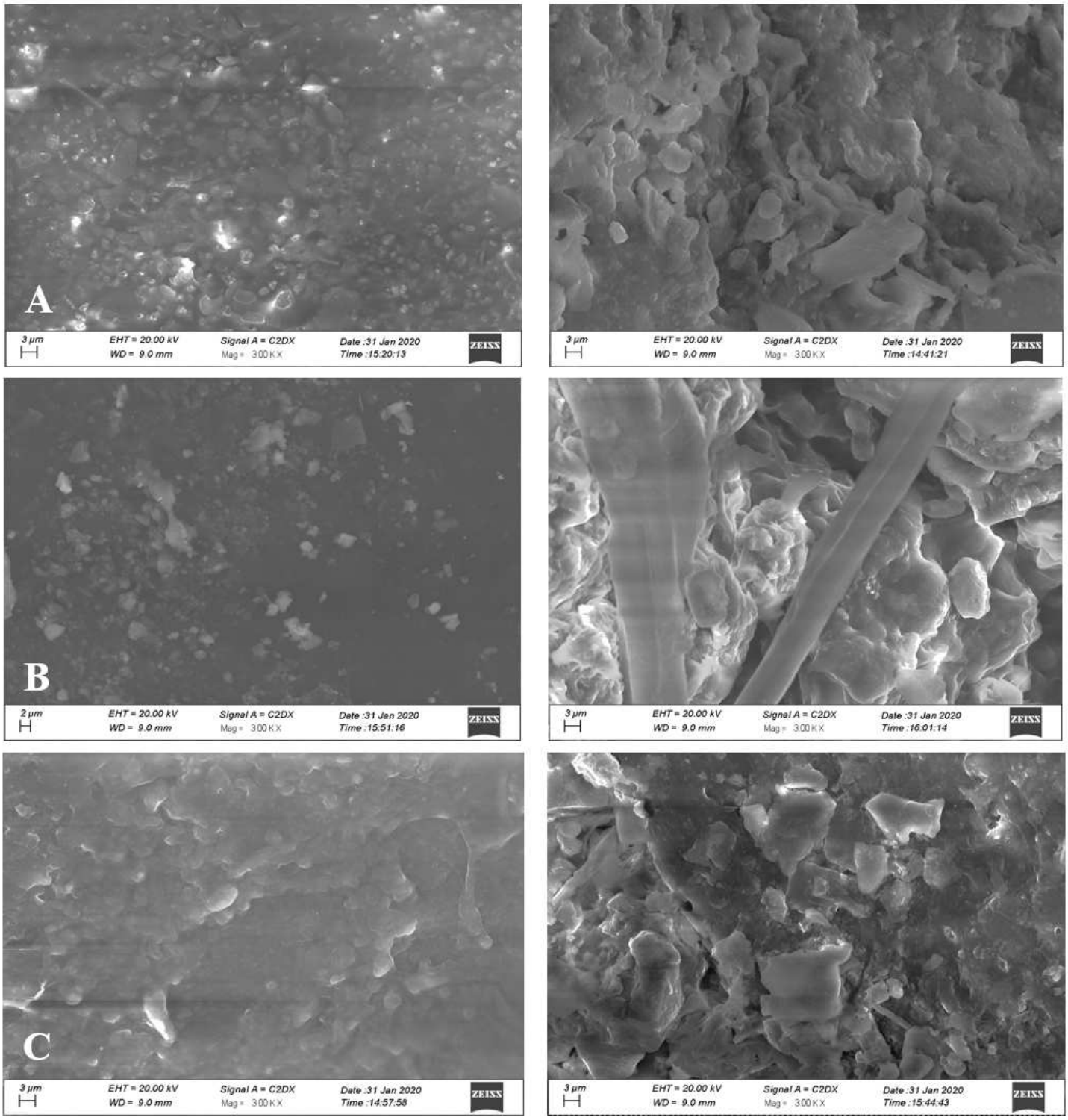

Figure 6

SEM of PHA sample F (A), PLA (B) and PHA-PLA sample PF (C) before and after degradation at 3000 X.

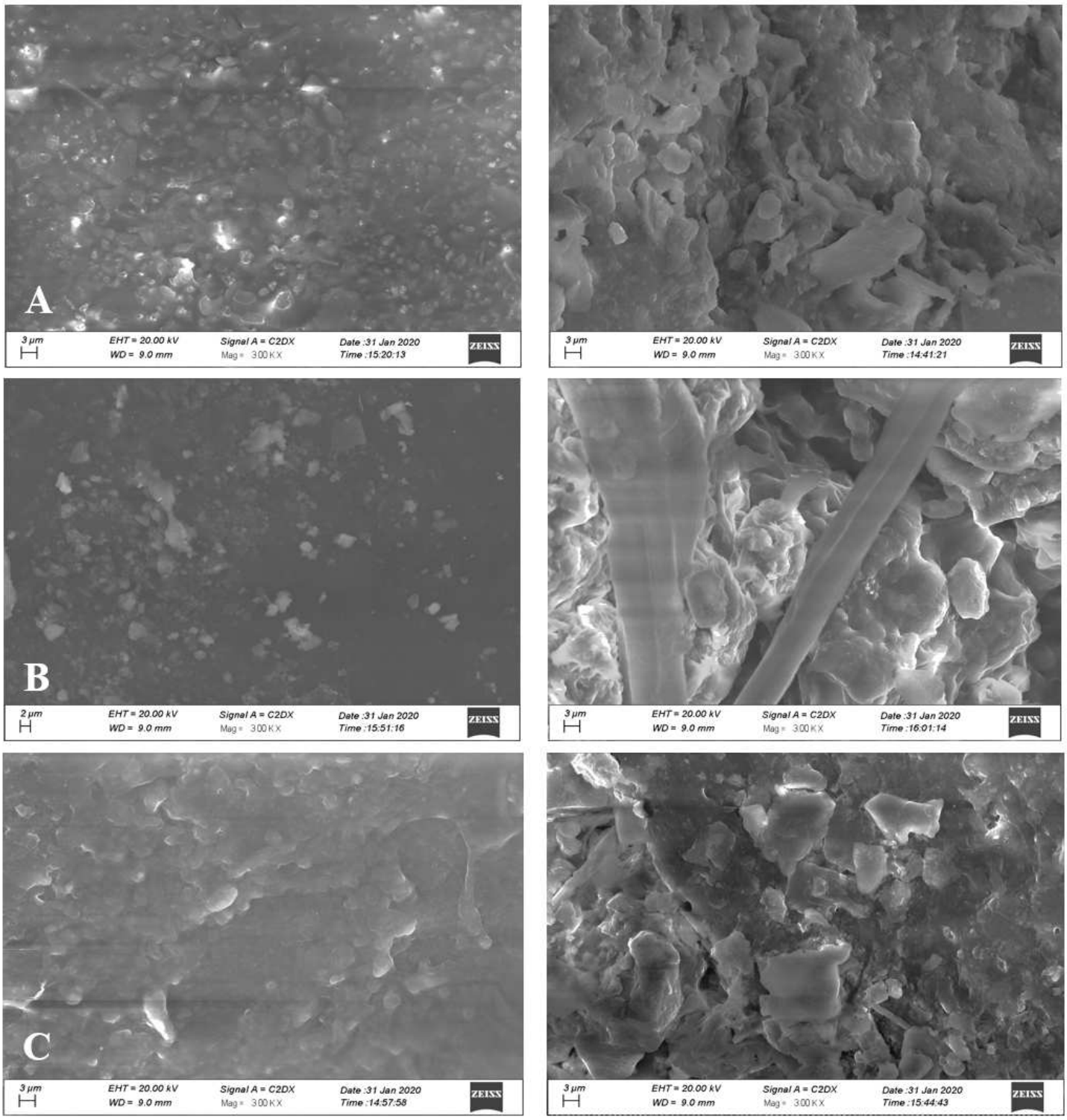

Figure 6

SEM of PHA sample F (A), PLA (B) and PHA-PLA sample PF (C) before and after degradation at 3000 X.

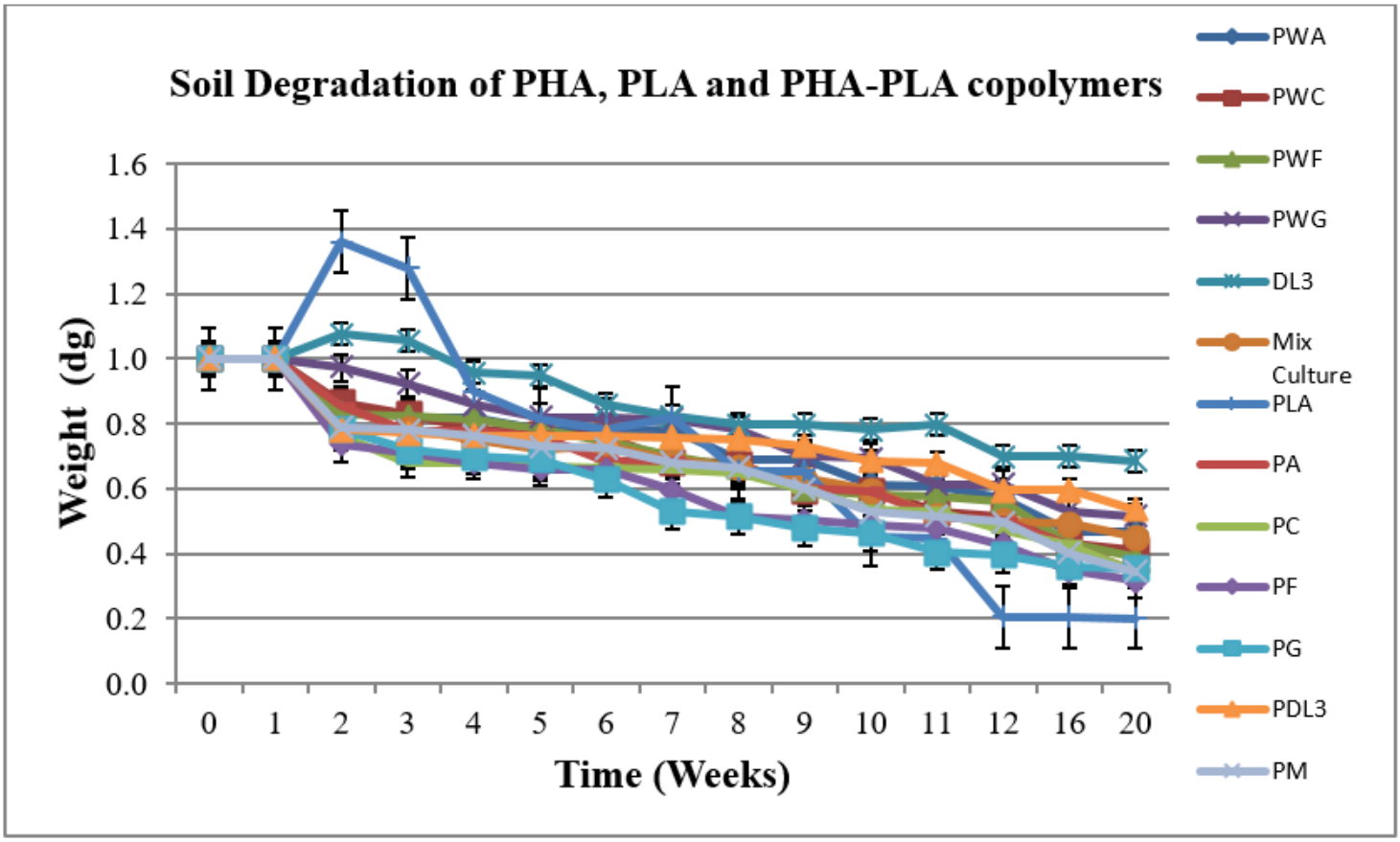

Figure 7

Graphical representation for soil degradation of PHA, PLA, and PHA-PLA blends.

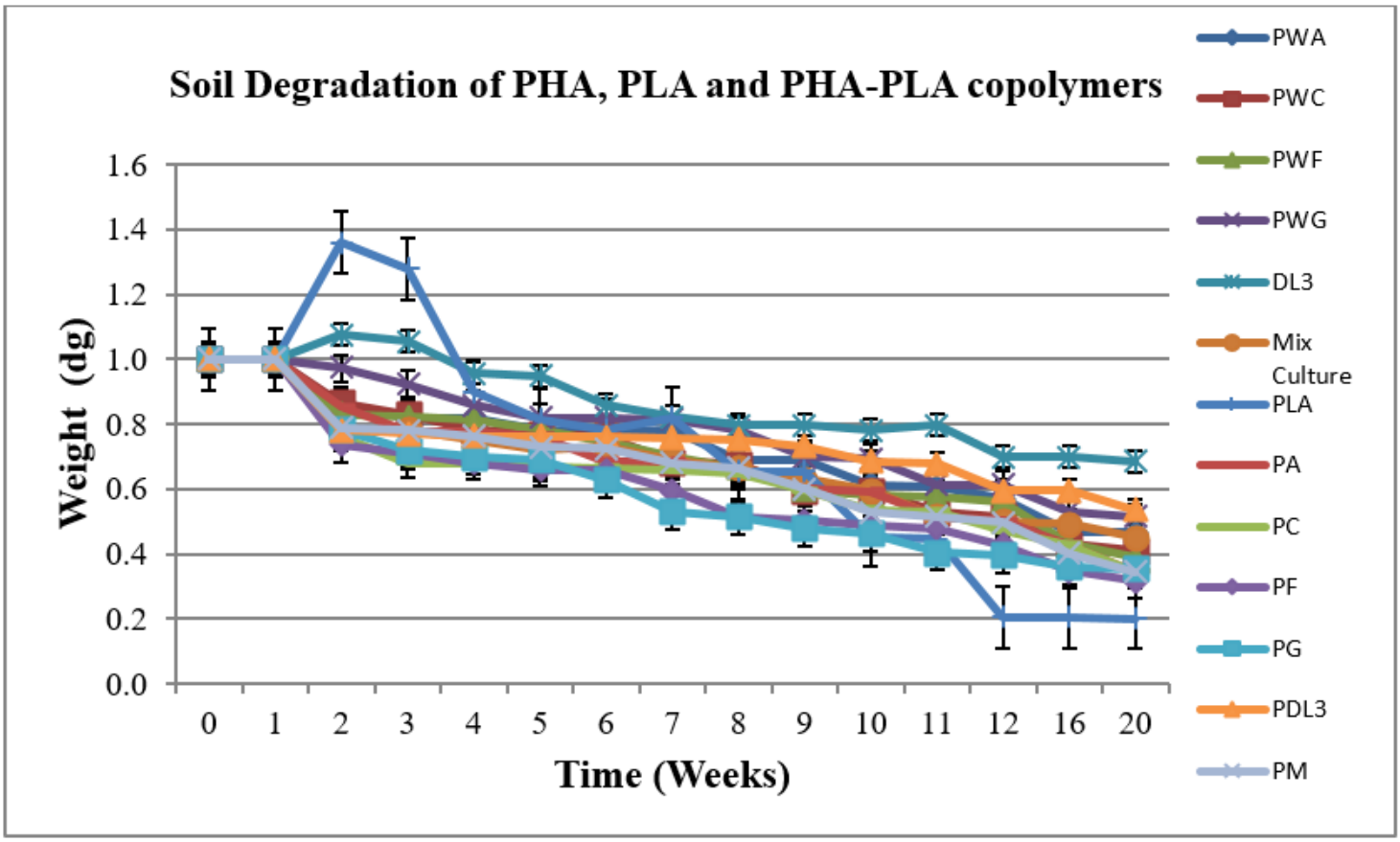

Figure 7

Graphical representation for soil degradation of PHA, PLA, and PHA-PLA blends.

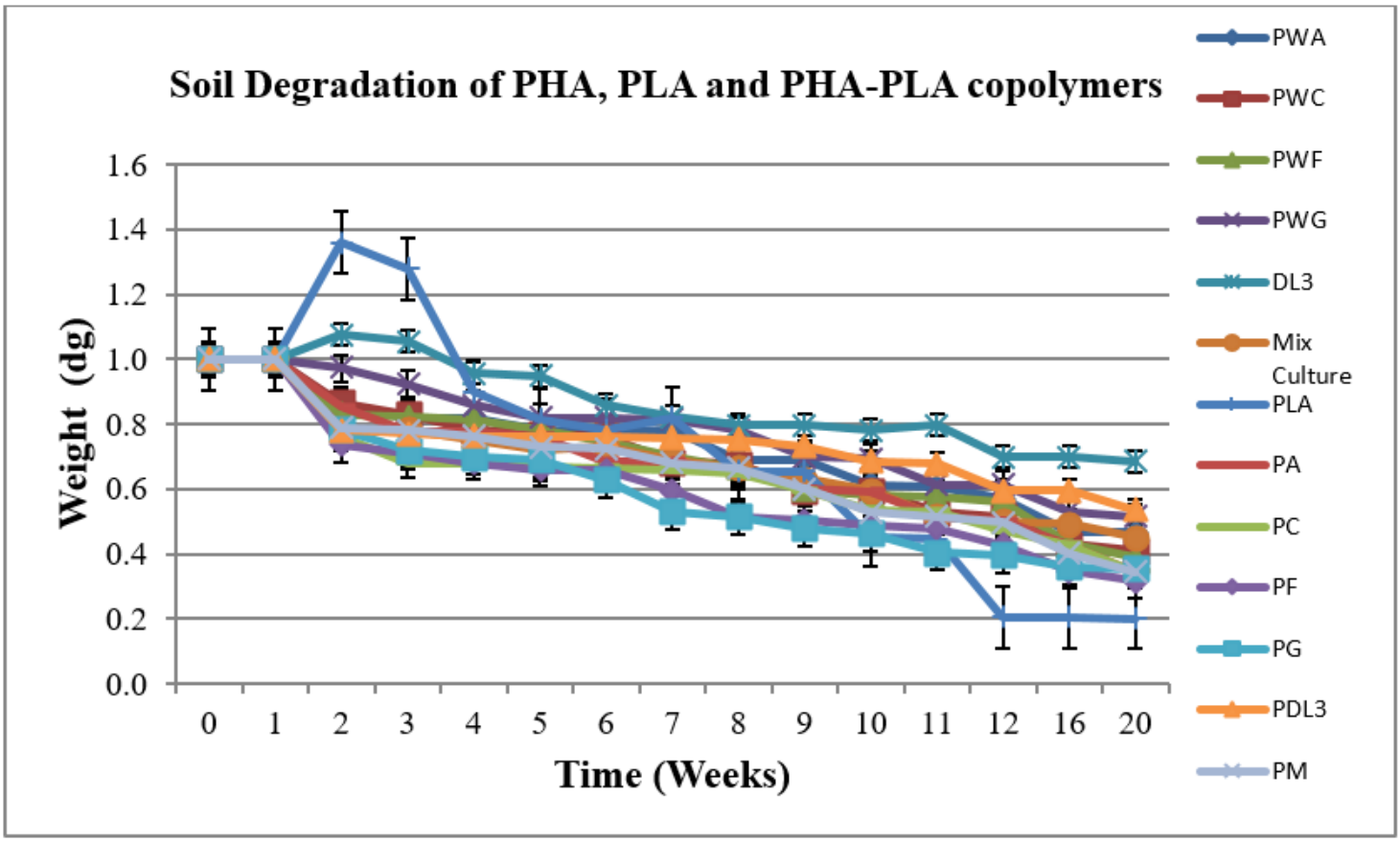

Figure 7

Graphical representation for soil degradation of PHA, PLA, and PHA-PLA blends.

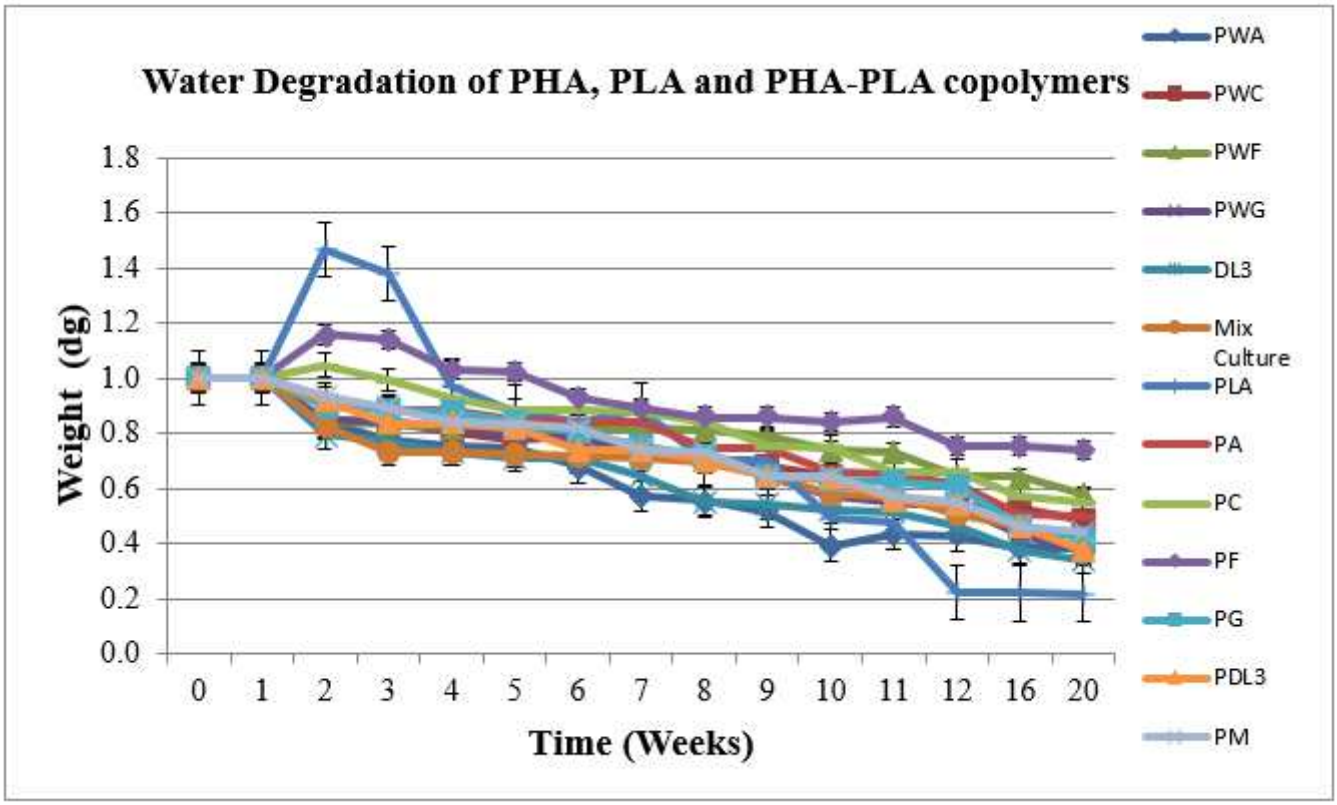

Figure 8

Graphical representation for water degradation of PHA, PLA, and PHA-PLA blends.

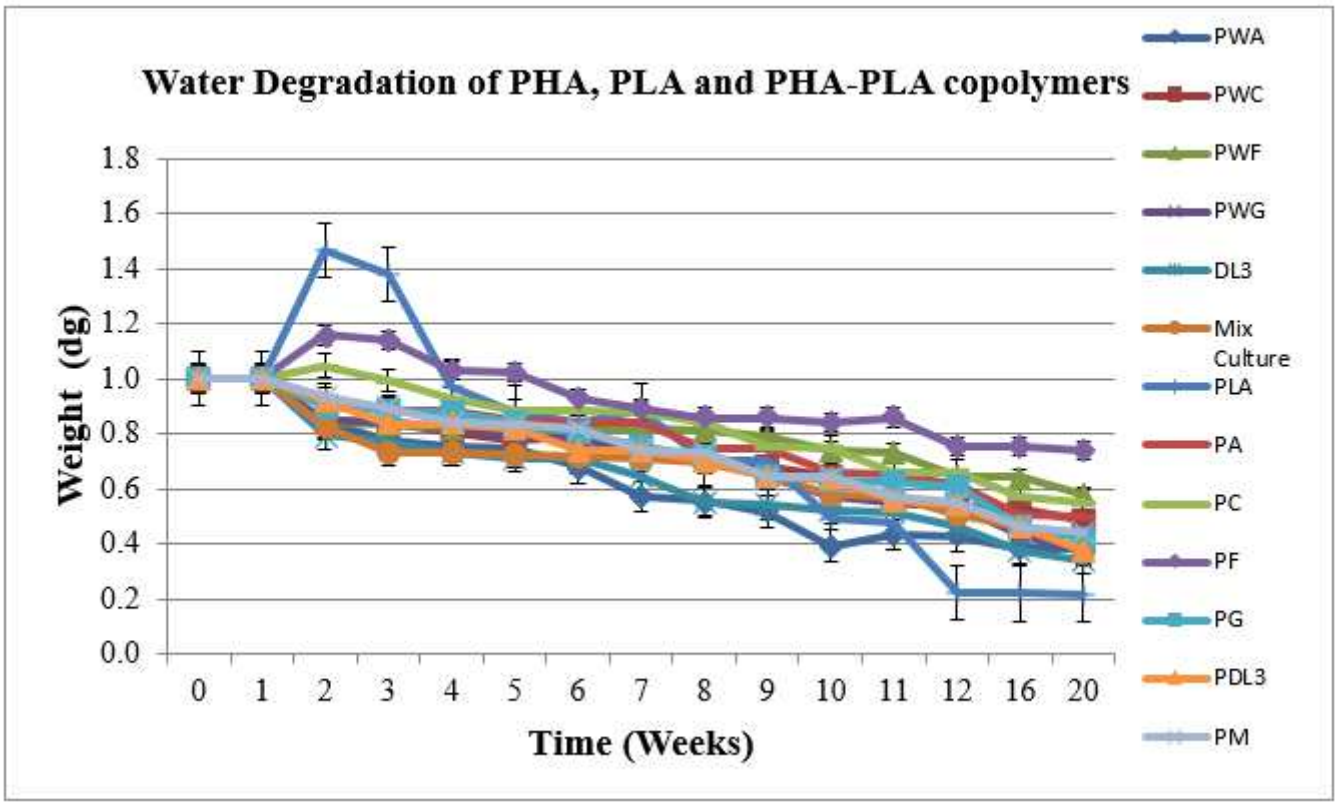

Figure 8

Graphical representation for water degradation of PHA, PLA, and PHA-PLA blends.

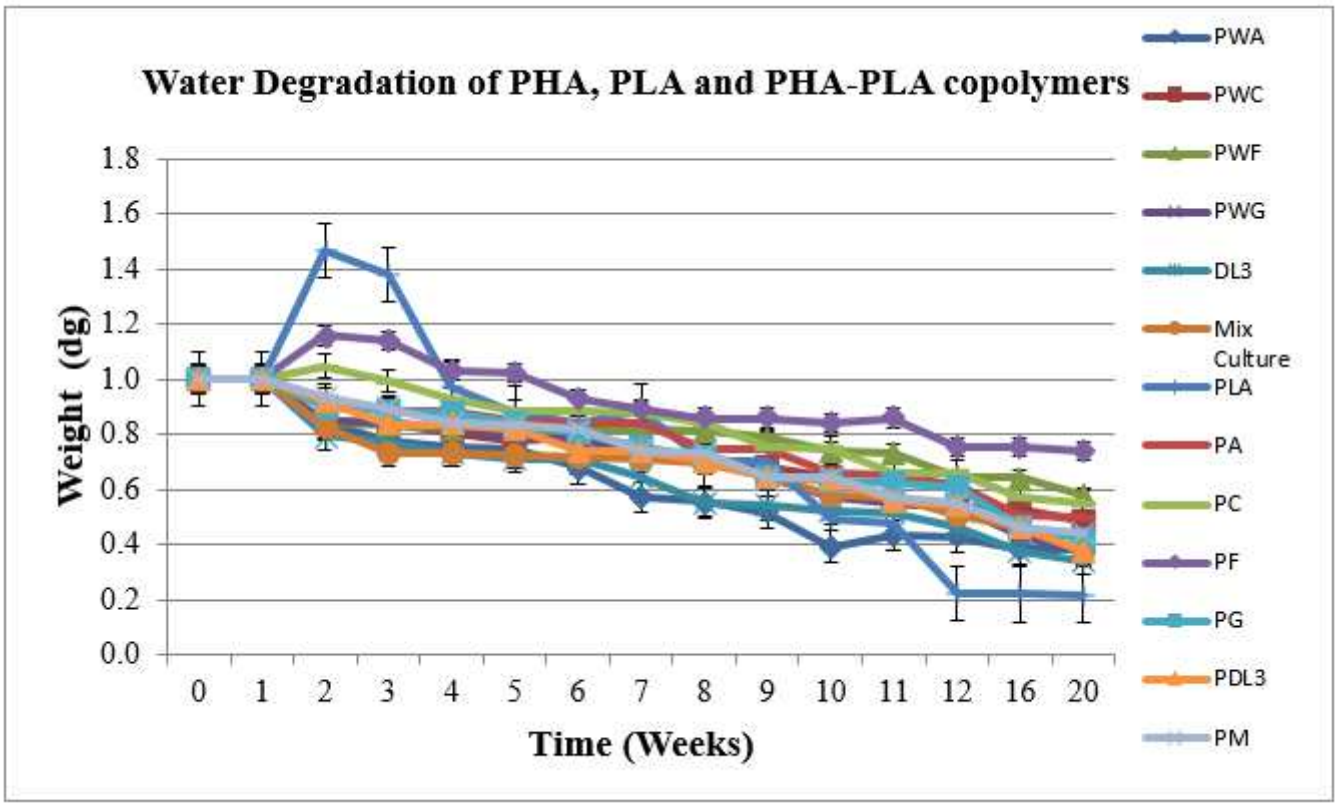

Figure 8

Graphical representation for water degradation of PHA, PLA, and PHA-PLA blends.

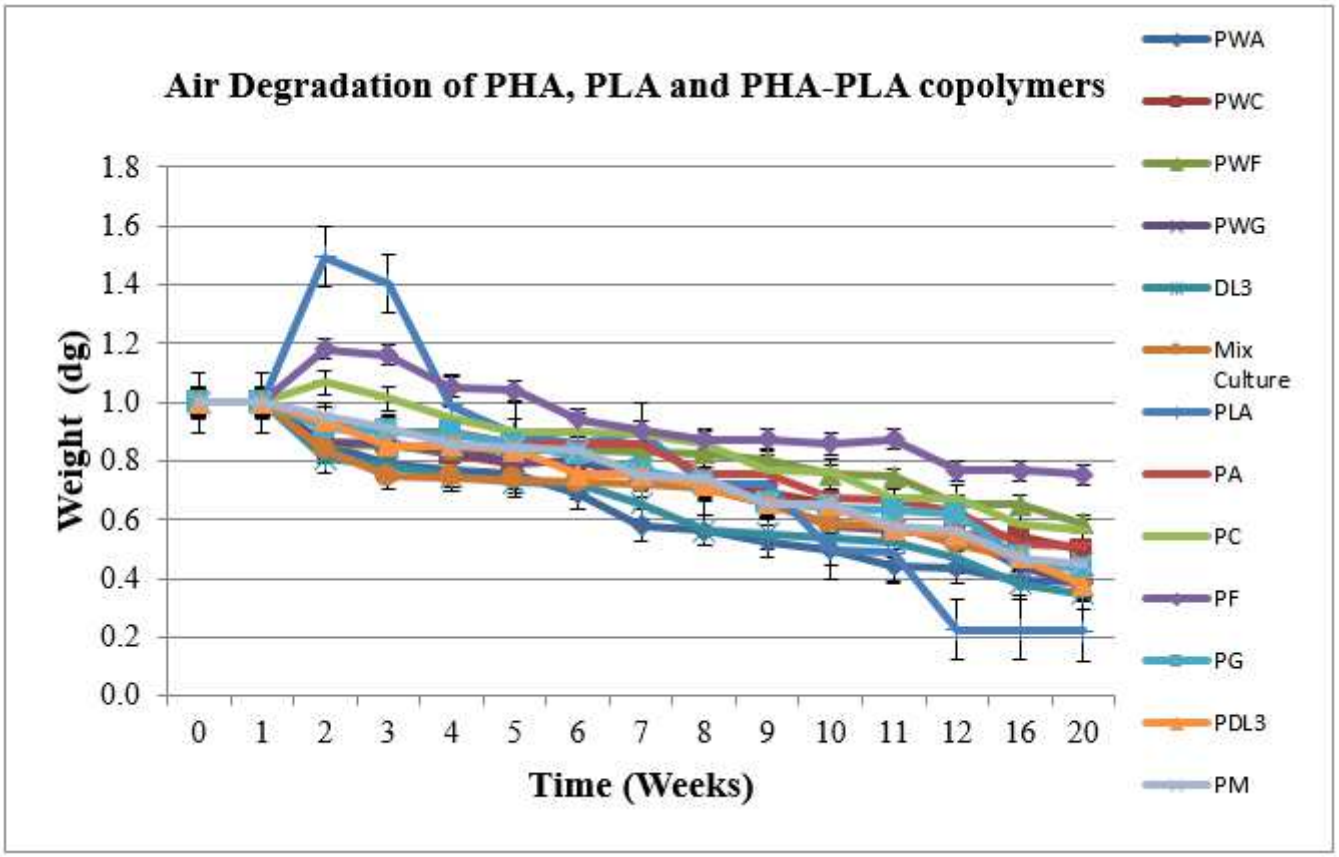

Figure 9

Graphical representation for air degradation of PHA, PLA, and PHA-PLA blends.

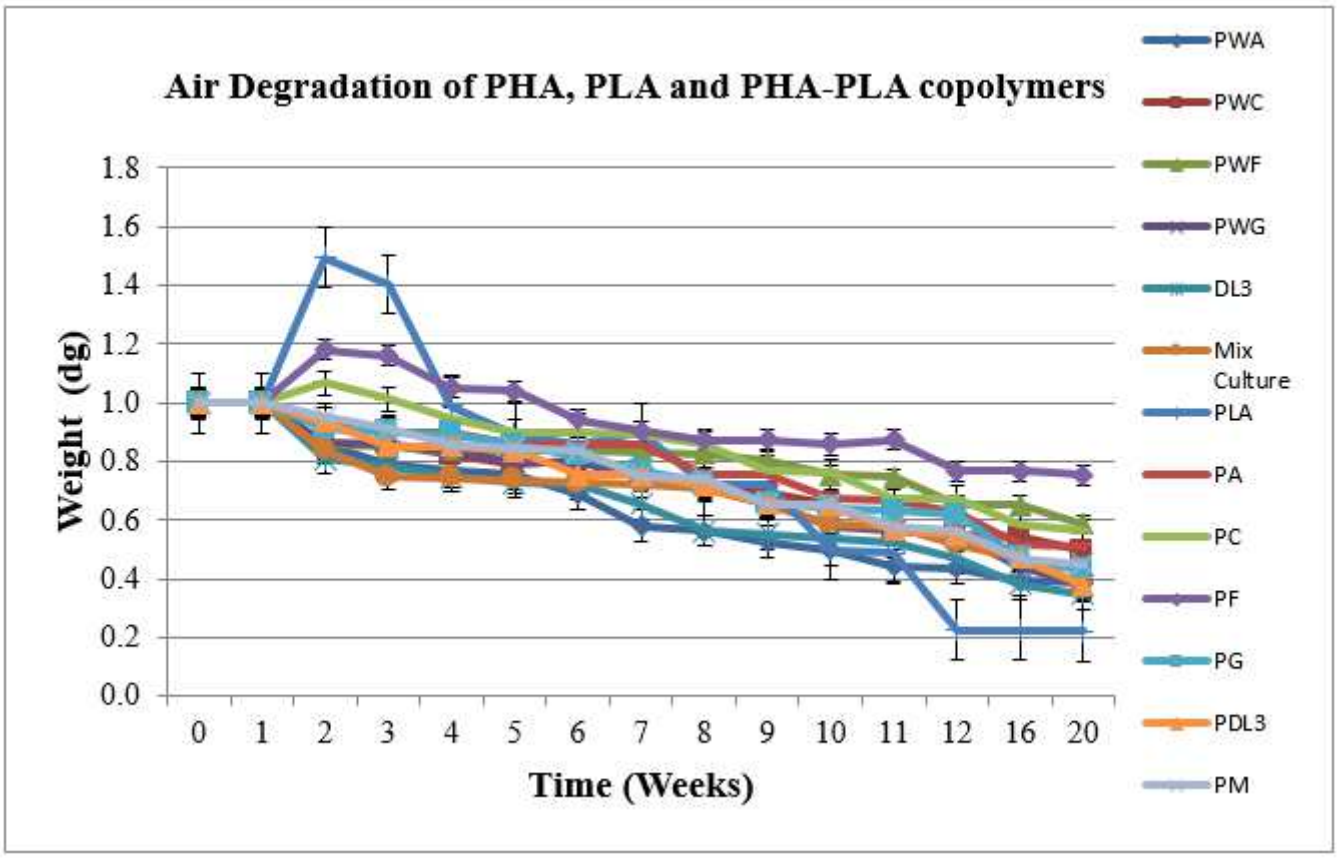

Figure 9

Graphical representation for air degradation of PHA, PLA, and PHA-PLA blends.

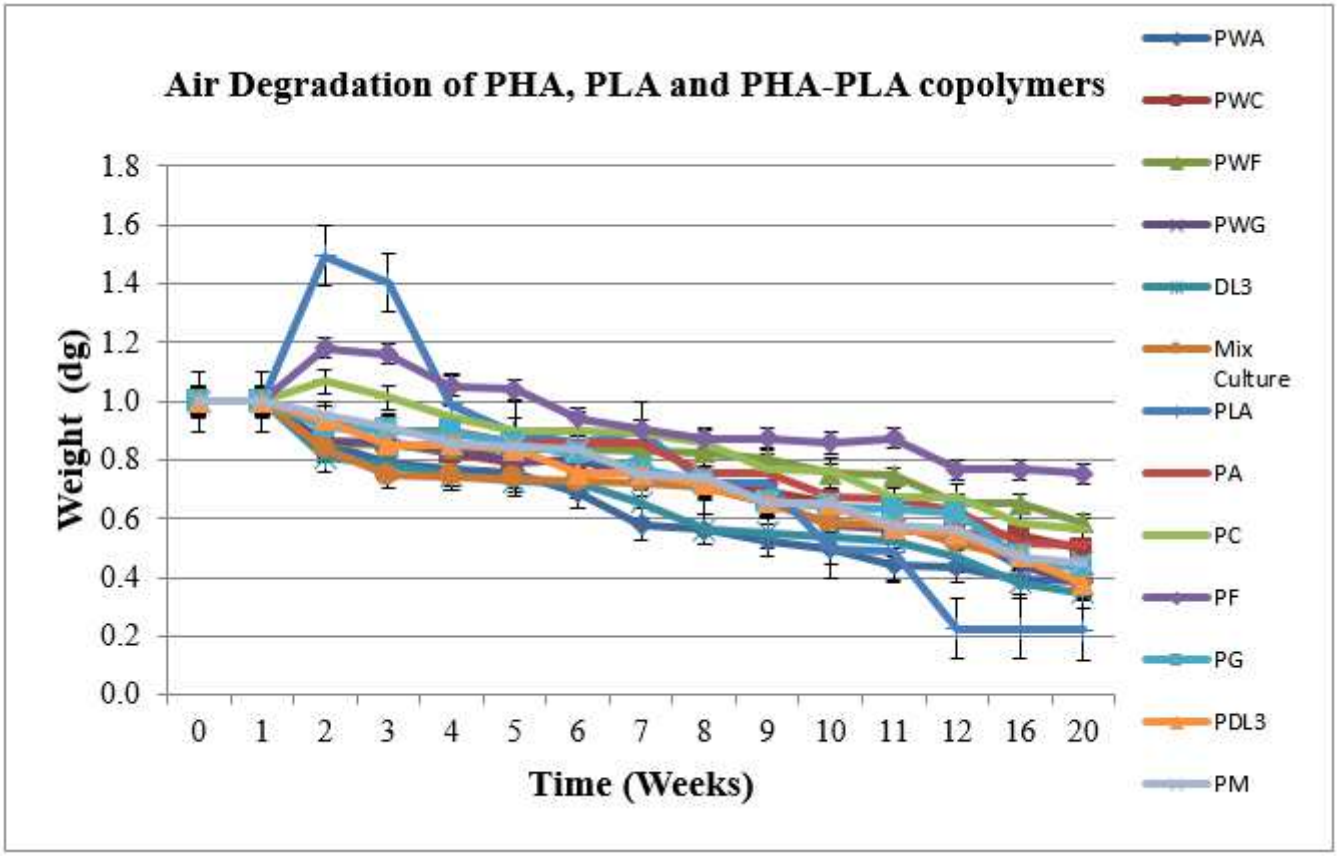

Figure 9

Graphical representation for air degradation of PHA, PLA, and PHA-PLA blends.

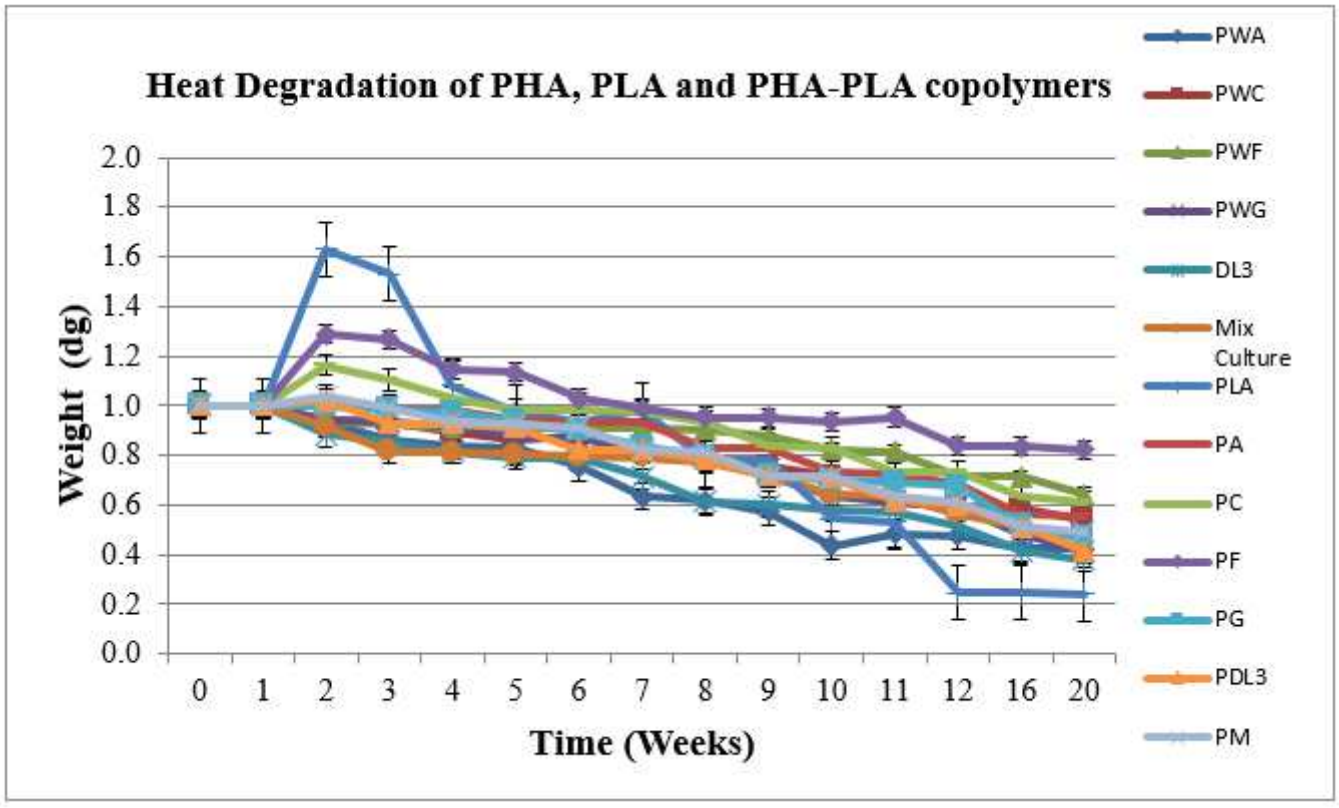

Figure 10

Graphical representation for heat degradation of PHA, PLA, and PHA-PLA blends.

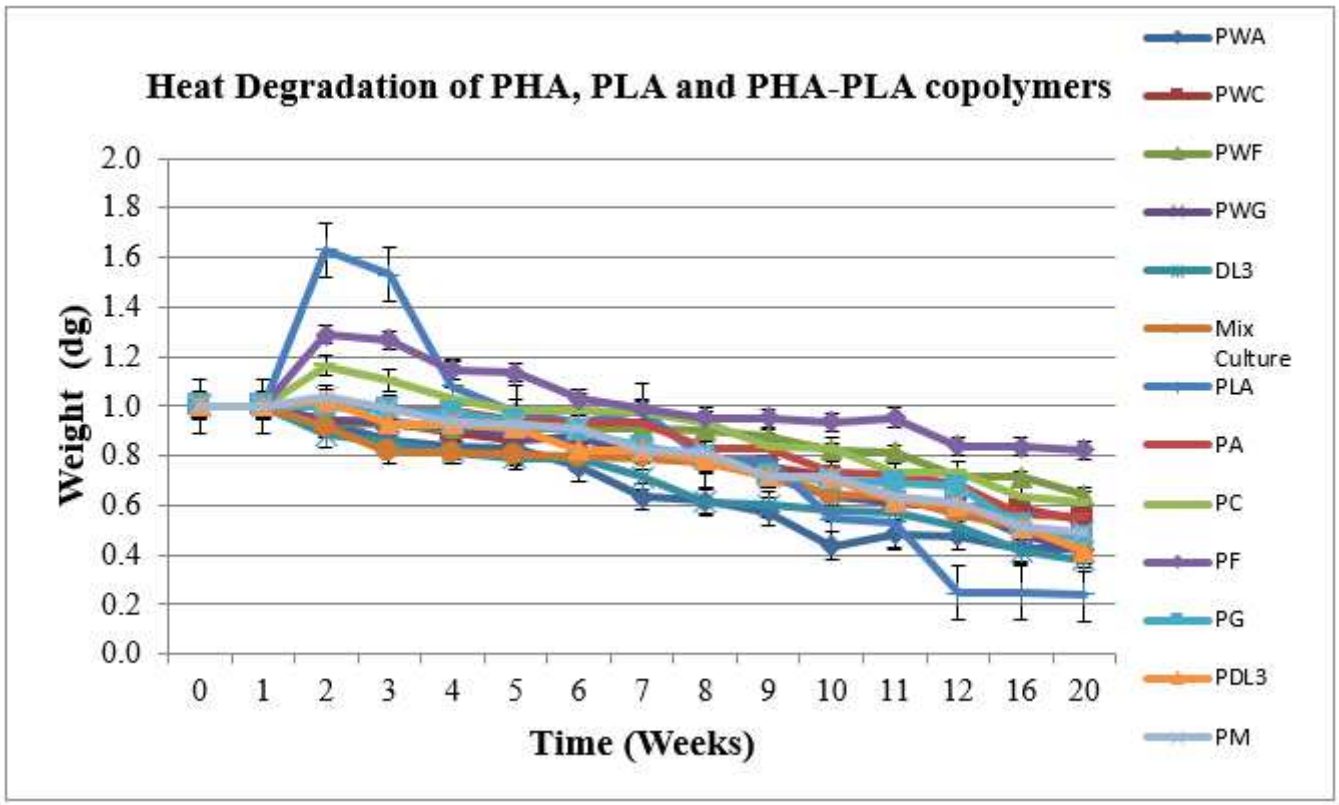

Figure 10

Graphical representation for heat degradation of PHA, PLA, and PHA-PLA blends.

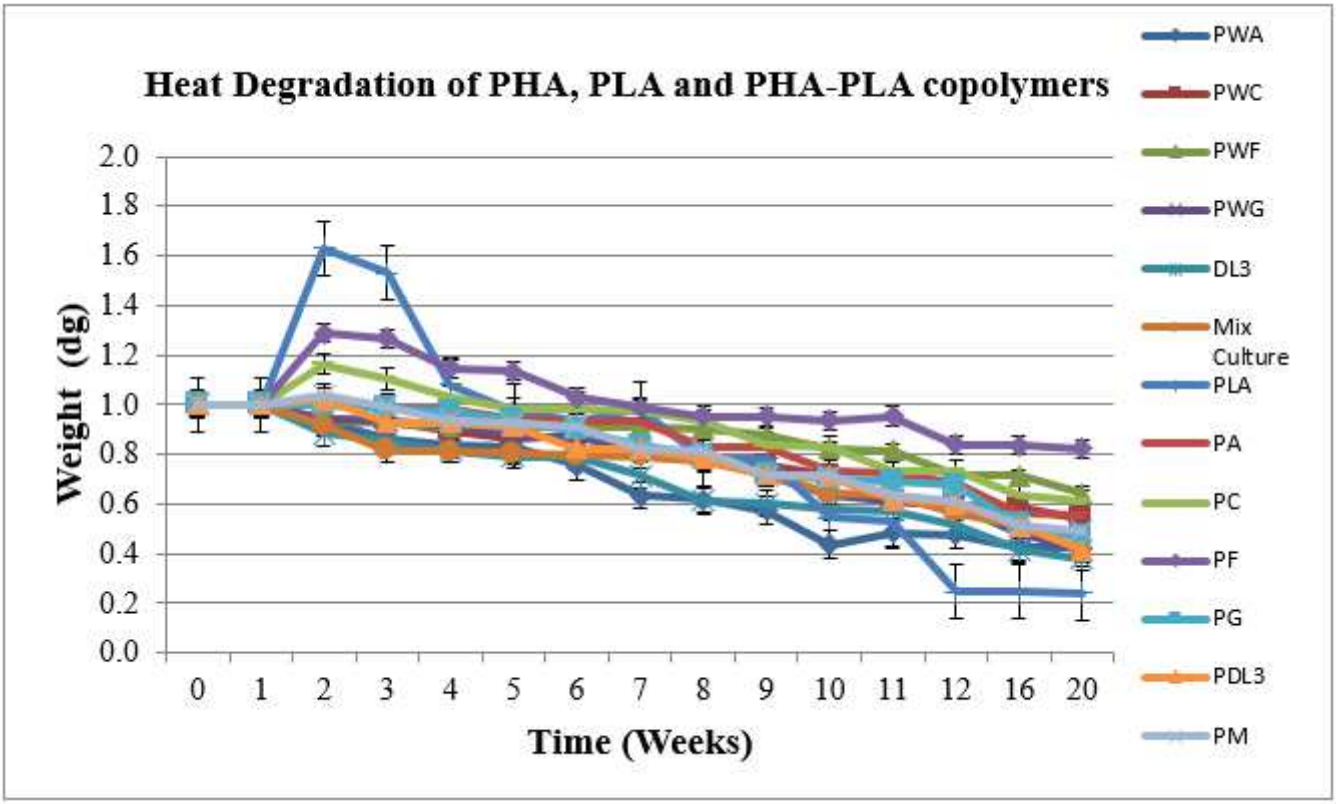

Figure 10

Graphical representation for heat degradation of PHA, PLA, and PHA-PLA blends.

Supplementary Files

This is a list of supplementary files associated with this preprint. Click to download.

- GraphicalAbstract.jpg
- GraphicalAbstract.jpg
- GraphicalAbstract.jpg